Published in final edited form as:
Dev Biol. 2009 May 15; 329(2): 242–257. doi:10.1016/j.ydbio.2009.02.024.

AGGRECAN MODULATION OF GROWTH PLATE MORPHOGENESIS

Miriam S. Domowicz, **Mauricio Cortes**, **Judith G. Henry**, and **Nancy B. Schwartz**[#]
Departments of Pediatrics and Biochemistry & Molecular Biology Committee on Developmental Biology The University of Chicago Chicago, IL 60637

Abstract

Chick and mouse embryos with heritable deficiencies of aggrecan exhibit severe dwarfism and premature death, demonstrating the essential involvement of aggrecan in development. The aggrecan-deficient nanomelic (nm) chick mutant E12 fully formed growth plate (GP) is devoid of matrix and exhibits markedly altered cytoarchitecture, proliferative capacity, and degree of cell death. While differentiation of chondroblasts to pre-hypertrophic chondrocytes (IHH expression) is normal up to E6, the extended periosteum expression pattern of PTCH (a downstream effector of IHH) indicates altered propagation of IHH signaling, as well as accelerated down-regulation of FGFR3 expression, decreased BrdU incorporation and higher levels of ERK phosphorylation, all indicating early effects on FGF signaling. By E7 reduced IHH expression and premature expression of COL10A1 foreshadow the acceleration of hypertrophy observed at E12. By E8, exacerbated co-expression of IHH and COL10A1 lead to delayed separation and establishment of the two GPs in each element. By E9, increased numbers of cells express P-SMAD1/5/8, indicating altered BMP signaling. These results indicate that the IHH, FGF and BMP signaling pathways are altered from the very beginning of GP formation in the absence of aggrecan, thereby inducing premature hypertrophic chondrocyte maturation, leading to the nanomelic long bone growth disorder.

Keywords

aggrecan; nanomelic; growth plate; hypertrophic chondrocyte; collagen; Indian hedgehog; osteopontin; osteocalcin; Fibroblast growth factor

INTRODUCTION

Growth and development of the long bones of the skeleton is a complex, multi-step, precisely-timed and spatially-organized process regulated by several genetic, endocrine and mechanical programs. During limb formation, mesenchymal cells migrate to establish areas of high cell density in a condensation process; at this stage the position, number and shape of the future skeletal elements is determined. After differentiation of mesenchymal cells into chondrocytes, development of cartilage occurs by both interstitial and appositional growth into the shape of future bone (Cohen, 2000a; Cohen, 2000b; Karsenty, 2003). Endochondral bone growth occurs

#To whom correspondence should be addressed at: Department of Pediatrics University of Chicago 5841 S. Maryland Ave., MC 5058 Chicago, IL 60637 n-schwartz@uchicago.edu Telephone: 773/702-6426 FAX: 773/702-9234.

in the epiphyseal growth plate (GP), a specialized tissue found at the ends of long bones. In this process, chondrocytes become arranged in columns parallel to the longitudinal axis of the long bones and differentiate, forming histologically distinct zones. Closest to the epiphyseal end of the GP are resting chondrocytes, which are metabolically less active. Next is a zone of proliferation in which cells only divide with cleavage planes perpendicular to the longitudinal axis of the long bone, hence the length of the column of cells increases (Cohen, 2000a; Cohen, 2000b). After several mitoses, chondrocytes mature, become encased in an extracellular matrix (ECM) and acquire a characteristic round morphology (pre-hypertrophic). In a further transition, the chondrocytes cease to divide, gradually increase in size and eventually hypertrophy. Ultimately, the hypertrophic chondrocytes die by apoptosis and are replaced by mineralized bone and bone marrow via vascular invasion, resorption of the cartilaginous matrix and recruitment of osteoblasts that deposit a bone-specific matrix (Horton, 1993; Horton et al., 1998; Olsen et al., 2000). This general paradigm is followed in both avian and mammalian GP development, with the exception that vascular penetration and GP erosion is less uniform in chick (Bruder and Caplan, 1989).

Concomitant with this series of morphological events, a highly-regulated gene expression profile is observed, involving an increasingly numerous array of growth regulators, transcription factors and signaling molecules that presumably are responsible for orchestrating the cellular and molecular events that direct the formation, maturation and eventual destruction of the transient cartilage, as well as for regulating expression of several matrix components that define the milieu surrounding the chondrocytic cell-types as they differentiate (Wagner and Karsenty, 2001). Of documented importance to this process is the expression of ECM molecules which provide structural support to the chondrocytes and likely either interact directly with the cells or create a milieu which affects passage from cell to cell of vital growth factors and signaling molecules. The ECM is composed predominantly of several types of collagens and proteoglycans, hyaluronan and link protein, with smaller amounts of other matrix-specific proteins (Schwartz and Domowicz, 2002a). Collagens provide the ECM with strength, elasticity and cohesion while the proteoglycans confer compressibility, resilience and form a gel-like medium that allows permeation by nutrients and other diffusible solutes (Wight et al., 1991), acting as a selective diffusion barrier (Quinn et al., 2001).

During skeletal development different proteoglycans are expressed in a highly-defined pattern that is regulated spatially and temporally. Versican, a large chondroitin sulfate proteoglycan (CSPG), is expressed in the undifferentiated mesenchymal cells of the early limb bud and during the onset of pre-chondrogenic condensation, then disappears with the differentiation to chondrocytes (Kimata et al., 1986). Concomitantly with the down-regulation of versican, a dramatic up-regulation of aggrecan, a biochemically similar member of this gene family, occurs during the establishment and maturation of the chondrocyte phenotype (Schwartz et al., 1993). Although other minor proteoglycans are produced by chondrocytes, aggrecan represents the bulk of the proteoglycan expressed during endochondral differentiation. Aggrecan interacts with filaments of hyaluronan to form aggregates which are further stabilized by interaction with link protein (Hardingham and Muir, 1973). Chondrocytes organize their pericellular matrix, composed largely of type II collagen and aggrecan; its assembly and retention at the surface of the cells is facilitated by the aggrecan-hyaluronan aggregate interacting with a cell-surface receptor, CD44 (Knudson and Knudson, 2001).

Mutations that affect the highly-organized processes of cartilage formation and endochondral ossification result in a host of inherited skeletal disorders, known as the chondrodysplasias. There are multiple loci at which mutations may affect proteoglycan-based phenotypes; i.e., genes for the core proteins, glycosaminoglycan-modifying and polymerizing enzymes, and signaling, growth and transcription factors that regulate synthesis and secretion of proteoglycans (Schwartz, 2002). In particular, mutations in the aggrecan gene in humans have

been associated with spondyloepimetaphyseal dysplasia with premature and severe osteoarthritis (Gleghorn et al., 2005; Tompson et al., 2009). Despite the continuing identification of proteoglycan defects associated with several chondrodysplasias (Schwartz, 2004; Schwartz and Domowicz, 2002a), there remains limited understanding of the underlying molecular mechanisms which lead to the altered GP phenotype.

We elucidated the first aggrecan core protein mutation in the homozygous recessive nanomelic (nm) chick (Li et al., 1993), which results in an extreme form of micromelia with reduced head and trunk size and gross skeletal abnormalities including extremely short, broad and malformed limbs. Homozygous nm embryos exhibit a rather homogeneous GP cell population, devoid of matrix and with loss of growth zone demarcation (Schwartz and Domowicz, 1998; Schwartz and Domowicz, 2002b; Schwartz and Domowicz, 2004). The nm mutants are morphologically indistinguishable from the wild type prior to embryonic day 8 (E8), and the fact that the number of skeletal elements is not changed indicates that this mutation does not alter the early determinants of the pattern formation process, but rather interferes with the growth of individual elements. These morphological observations suggest several possible consequences of the matrix deficiency underlying the disorganized GP in the nm mutant; e.g. normal chondrocyte differentiation may be altered because aggregan is a key factor in controlling maturation, or the process of bone formation may be accelerated because aggrecan acts as an anti-angiogenic factor in the matrix. Alternatively, the observed phenotype may be due an altered diffusion or selective-permeability barrier because of the absence of aggrecan in the ECM which could affect growth factor diffusion and/or morphogen gradient formation. To begin to address these issues, the gene expression patterns of relevant matrix and GP-specific molecules were analyzed concomitantly with a detailed analysis of the GP developmental steps which are influenced by the lack of aggrecan.

MATERIALS AND METHODS

Wild type (wt) fertilized White Leghorn chicken eggs were purchased from Sharp Sales (West Chicago, IL). Fertilized eggs from nanomelia heterozygote (+/nm) crosses were provided by the Department of Animal Genetics, University of Connecticut (Storrs, CT). Eggs were incubated at 37.9°C at 60% humidity in a Midwest incubator with automatic egg turning, regularly hatching at day-21 of incubation. In all experiments, both White Leghorn embryos and embryos of normal progeny from the nanomelia heterozygote crosses (flock-mates) were tested as controls. No differences between these two set of controls were found in the levels, distributions and developmental regulation of any messages assayed by *in situ* hybridization or immunocytochemistry. Affected embryos (−/−) could be detected morphologically by E8 while early identification was done by genotyping (Li et al., 1993).

Immunocytochemical staining

Limbs from chick embryos were fixed at 4°C with fresh 4% paraformaldehyde in phosphate-buffered saline (PBS), then embedded in paraffin for sectioning. Tissue sections (10 μm) were dewaxed in xylene, rehydrated by passage through a series of decreasing-percentage ethanol solutions, then treated with 5 mg/ml bovine serum albumin for 1 h to block nonspecific binding prior to overnight incubation with the anti-aggrecan monoclonal antibody S103L (1: 100 dilution). After extensive washes with PBS, sections were incubated for 2 h in alkaline phosphatase-conjugated secondary antibody solution (AP-anti-rat IgG from Pierce diluted 1:100), washed again with PBS, mounted in Eukitt mounting medium, and photographed with a Nikon microscope. For P-SMAD1/5/8 and P-SMAD2 immunostaining, Chemicon antibodies were used after unmasking epitopes by treating the sections with 0.1M citric acid pH 6 for 15 min in the microwave. The peroxidase signal was amplified with tyramide-FITC.

P-SMAD-positive nuclei from limb sections were counted and the counts standardized for the number of DAPI-positive nuclei using ImageJ software. Data was analyzed for statistical significance using the Student's *t*-test.

PCNA immunostaining was performed following a similar procedure using the PC10 antibody from DAKO (1:250 dilution). Photographs (6-8) of the hypertrophic and proliferative zones from multiple limb elements were used for quantification. Statistical analysis was performed using the Student's *t*-test. Apoptosis was assessed *in situ* using the TUNEL method (Tdt-mediated dUTP nick-end labeling) (Brunner, 1998). Alternatively, for proliferation assays BrdU (1.6 mg/100 μl) was applied to the vitelline membrane of E18 eggs 3h prior to tissue harvest. Tissue was then fixed, embedded, sectioned and processed for immunocytochemistry using an anti-BrdU IgG (BD Bioscience) primary antibody and alkaline phosphatase conjugated anti-rabbit IgG (Roche, Germany) secondary antibody.

Von Kossa's stain

Limbs fixed in 4% paraformaldehyde/PBS were mounted in paraffin and 10 μm sections were cut and treated with 2% silver nitrate solution; the matrix-bound calcium was then reduced by exposure to strong light and replaced with silver deposits (Thompson and Hunt, 1966). Sections were counterstained with hematoxilin.

mRNA in situ hybridization

E12 chick limbs were fixed in 4% paraformaldehyde/PBS overnight. The tissue was sunk in 20% sucrose/ 10% formalin in PBS, embedded in 10% gelatin / 20% sucrose and sectioned at a thickness of 40 μm. Sections were mounted on Superfrost/Plus microscope slides (Fisher) pre-coated with poly-L-lysine. Slides were processed for non-radioactive *in situ* hybridization as previously described (Domowicz et al., 2008). Two-color fluorescence *in situ* hybridization (FISH) was performed on E9 limb sections as previously described (Domowicz et al., 2008).

Western blotting

Lysates from E6 wt and nm cartilage were prepared in RIPA buffer with phosphatase and protease inhibitors (PhosSTOP and Complete from Roche). Total protein was normalized using the BCA assay (Pierce) and equal amounts of protein were subjected to 10% SDS-PAGE and electrotransferred to nitrocellulose membrane at 150mA overnight. Primary antibodies used are anti-β-actin (mouse IgG, 1:1000, Sigma) and anti-Phospho-p44/42 MAP Kinase (Rabbit IgG 1:1000, Cell Signaling), and the secondary antibody was a HRP-conjungated goat anti-mouse IgG and anti-rabbit IgG (Pierce), respectively. Signal was detected using the SuperSignal West Dura Extended Duration Substrate (Pierce) and visualized and quantified by Quantity One software (Bio-Rad).

cDNAs

Aggrecan gene expression was analyzed with riboprobes derived from a 690-bp fragment from exon 12 of the chicken aggrecan gene, obtained as previously described (Domowicz et al., 2008) Probe fragments for IHH, COL10A1, COL2A1, osteopontin and osteocalcin were obtained by PCR from a cDNA library generated using random hexamer primers, E12 chick cartilage mRNA and SuperscriptII-Reverse Transcriptase (Invitrogen). The specific PCR primers used were GACTGCGTGGTGAGAGAGG-3' and TGGCTCTAACGGCATGC-3' for COL2A1; ATGCTCGCAGTGCTAAAGCCT-3' and AGAAGTGGAGCATAATGGGGG-3' for osteocalcin; CATTGCTGCTGCATGGCC-3' and GCTGGCGTCGACGGCGG-3' for osteopontin; CCAACGTGCCCGAGAAGA-3' and AGTGGATGTGCGCCTTGGA-3' for IHH; GGGTGAAGAAGGGG-3' and TGGTAAACCTGGC-3' for COL9A1; AGAAGAATGAAC-3' and ATCCCAGAAGG-3' for COL10A1. Chick PTHrP receptor and

BMP6 cDNA fragments were generated in similar fashion using degenerate primers based on the known human and mouse sequences. Degenerate oligonucleotides were designed with the aid of the Blocks and CODEHOP (COnsensus-DEgenerate Hybrid Oligonucleotide Primers) programs (http://blocks.fhcrc.org/) (Rose et al., 1998). The specific primers used were TCCTGAACGACGCCgayatggtnatg-3' and TGGGGGCGATGAtccartcytgcc-3' for BMP6 and CCCGACTACATCTACGACTTCaaycayaargg-3' and GCACCGGCCGgcrttngtytc-3' for PTHrP receptor. PCR products were ligated into the pCRII dual-promoter vector plasmid from Invitrogen. Sequencing of the cloned gene fragments was performed with an ABI PRISM 377XL sequencer (Perkin Elmer) by the University of Chicago Cancer Center DNA Sequencing facility. Riboprobes incorporating DIG-labeled nucleotides were synthesized from linearized plasmid templates with T7 or SP6 polymerase (Roche). As controls, *in situ* hybridizations using probes for neurocan and brevican messages, which are not expressed in limbs, were performed with negative results.

Semi-quantitative RT-PCR

OneStep RT-PCR mix (Qiagen) was used to amplify target RT-PCR fragments according to the manufacturer's protocol, using 0.5 μg of total wt or nm E6 limb or E12 limb cartilage RNA. Cycling parameters for each PCR fragment were optimized by varying the annealing temperature, extension time and number of cycles (25-35) so that the amplification was in the exponential range. Amplified DNA was electrophoresed in on a 1.5% agarose gel, then imaged and quantified using the BioRad ChemiDoc XRS imaging system.

Embryonic limb explant cultures

Chicken tibia were stripped of skin and muscles by gentle rubbing against sterile filter paper and cultured in BGJ-B medium (Invitrogen) with penicillin/streptomycin (Invitrogen) and 0.1% BSA (Minina et al., 2001). Tibias from the same embryo were kept as matched pairs mach. Members of each pair was cultured with or without 10 μM cyclopamine (Incardona et al., 1998). After 48h in culture, explants were fixed, photographed and processed for mRNA in situ hybridization. Total tibial growth length was determined using ImageJ.

RESULTS

GP development in day-12 aggrecan-deficient nanomelic chick

In the epiphyseal GPs of mid-development (day 12) chick embryos, chondrocytes at progresive stages of differentiation are organized into well established architecturally distinct zones. Hematoxylin-eosin staining of embryonic day-12 chick limbs highlights abnormal morphological aspects of the proliferative and hypertrophic zones of nm epiphyseal cartilage compared to wild type (wt) (Fig. 1A & B) including: *i)* disruption of normal cytoarchitecture; *ii)* higher cell density per unit area; *iii)* absence of matrix between cells; *iv)* condensed nuclei, and *v)* smaller hypertrophic chondrocytes. The chick aggrecan-specific monoclonal antibody S103L exhibits abundant membrane-associated and ECM staining in the proliferative zone of wt cartilage, but only very faint (intracellular) staining in nm limb. In the hypertrophic zone, S103L-stained aggrecan is also abundant and predominantly extracellular in wt, while there is no reaction product in the mutant (Fig. 1, C & D), verifying complete absence of the aggrecan molecule.

Since cell-number homeostasis as well as the normal architecture of the GP result directly from a balance between cell proliferation and apoptosis, the rate of cell division and extent of cell death were independently assessed in the aggrecan-deficient mutant. When E12 wt limb sections were stained with an antibody to proliferation cell nuclear antigen (PCNA), which marks cells in the S-phase of the cell cycle, a large number of proliferative-zone cells were stained, while very few hypertrophic-zone cells were PCNA-positive. Interestingly, intense

staining with the PCNA antibody in both proliferative and hypertrophic chondrocytes was observed in the nm mutant (Fig. 1, E & F). Upon quantitative analysis, statistically significant increases were found in the number of S-phase cells per unit area sampled among nm proliferative (3-fold) and hypertrophic (20-fold) chondrocytes, compared to the respective wt regions (Fig. 1, I, PCNA-positive). Taking into account the increased number of cells per unit surface area in the nm cartilage compared to the wt (Fig. 1, total numbers), approximately 1 of every 5 chondrocytes in the wt proliferative zone undergoes cell division in a given time period while 1 of every 4 chondrocytes does so in the nm proliferative zone. While it is rare to observe a PCNA-positive cell in the wt hypertrophic zone, 1 of every 3 nm hypertrophic chondrocytes expresses PCNA. These results indicate an increased proliferative rate for nm chondrocytes in the absence of aggrecan in the matrix. Qualitatively, TUNEL staining of wt limbs showed that more cell death occurs among hypertrophic than proliferative zone chondrocytes, while in nm mutants there was a slight increase in the number of apoptotic cells in the hypertrophic zone and an unexpectedly greater increase in the proliferative zone (Fig. 1, G & H).

The significant abnormalities in chondrocyte morphology and homeostasis are reflected in the striking growth retardation observed in the E12 nm GP. (Fig. 2). Most notably, E12 nm tibias are approximately one-third the length of their wt counterparts, and the structure of the limbs are grossly distorted (Fig. 2A). GP zone demarcation in day-12 wt chick tibias is clearly indicated by expression of mRNAs for alpha 1 type IX collagen (COL9A1) (Fig. 2A & B), alpha 1 type II collagen (COL2A1) and alpha 1 type X collagen (COL10A1) (Fig. 2B). Except for the hypertrophic chondrocytes, all zones of the GP express COL9A1 and COL2A1, albeit to differing degrees. The terminal state of wt chondrocyte differentiation (hypertrophic) is accompanied by a significantly different profile of gene expression, typified by strong expression of COL10A1 (a marker of hypertrophic chondrocytes) transcripts and no further expression of COL9A1 and COL2A1 mRNAs (Fig. 2B). Further comparison of GP size in nm and wt E12 tibias on the basis of the extents of their COL10A1, COL9A1 and COL2A1 expression domains indicates that all regions are proportionally reduced in the mutant, again reflecting the dimensional differences in the long bones. Mapping of GP zones using these three well-characterized collagen components shows that states of chondrocyte differentiation are tightly coordinated with gene expression as previously illustrated (Sandell et al., 1991;Sandell et al., 1994;Wai et al., 1998), and thus can be used to correlate the expression patterns of other genes important to GP development in normal and chondrodystrophic limbs. In particular, when the expression pattern of aggrecan across the wt chick GP was analyzed (Fig. 2B), the levels of aggrecan expression vary with the state of chondrocyte differentiation; resting chondrocytes exhibit a low, steady level of aggrecan expression, while much higher levels of expression are observed for proliferative and pre-hypertrophic chondrocytes, followed by markedly reduced levels in the mature hypertrophic chondrocytes, similar to the COL2A1 and COL9A1 patterns. In contrast, significantly reduced levels of aggrecan mRNA expression are detected in all regions of nm cartilage, in agreement with previous findings by Northern analysis (Li et al., 1993). Despite the drastic reduction of aggrecan expression in nm cartilage, COL2A1 and COL9A1 are still strongly expressed, although in significantly reduced domains. Also note that even though levels of aggrecan message are largely reduced in wt hypertrophic chondrocytes, immunostaining with the aggrecan antibody S103L is still high (Fig.1 D). This persistence has been observed in mouse as well (Shibata et al., 2003) and likely is due to the slow turnover of the aggrecan protein (Mok et al., 1994).

Changes in regulatory-gene expression in aggrecan-deficient GP

The expression patterns of certain gene products, i.e. signaling molecules, growth factors and transcription modulators, previously shown to regulate epiphyseal GP formation were also assessed. While in serial sections of wt tibias (Fig. 4) there is clear demarcation of the areas

expressing COL10A1 (characteristic of hypertrophic chondrocytes) and Indian hedgehog (IHH) (characteristic of pre-hypertrophic chondrocytes), both markers are expressed in the same area in the nm mutant, making it impossible to distinguish the hypertrophic and pre-hypertrophic zones (Fig. 2B & 3A and 4). Even though the expression domain of IHH is greatly reduced in the mutant, levels of IHH mRNA expression remain unchanged compared to wt (Fig. 3 B). Osteopontin (OPN), a marker of late hypertrophic chondrocytes and osteoblasts, is partially co-expressed with COL10A1 in wt embryos, while in nm epiphyseal cartilage transcripts for OPN also co-localize with those for COL10A1 and IHH, and are present at increased levels in sites associated with secondary ossification (Fig. 3A, arrow). Osteocalcin (BGLAP), a marker of osteoblasts, is localized in comparable patterns in the trabecular bone associated with both wt and nm GPs. BMP6, a member of the bone morphogenetic protein family that is expressed predominantly in pre-hypertrophic chondrocytes (Solloway et al., 1998;Vortkamp et al., 1996), is observed in a pattern that partially overlaps that of IHH in wt embryos (Fig. 3A). A narrow band of BMP6 expression persists in nm GP, most likely marking newly-differentiated hypertrophic chondrocytes. However, BMP6 expression also overlaps the distal region of IHH expression and completely overlaps the area of COL10A1 expression. Previous studies have shown that the parathyroid hormone-related peptide (PTHrP) receptor (PTH1R) is expressed throughout the GP but at much higher levels in pre-hypertrophic chondrocytes proximal to the proliferative zone, while IHH is expressed at the pre-hypertrophic/hypertrophic zone boundary (Amizuka et al., 1994;Lee et al., 1995). Our gene expression screen in wt E12 embryos showed that PTH1R is indeed localized to pre-hypertrophic chondrocytes proximal to the proliferative zone and the adjacent perichondrium in wt E12 embryos (Fig. 3A). In nm embryos of the same age, a small region of PTH1R expression persists at the borders of the hypertrophic region near the perichondrium, but the level of PTH1R in the pre-hypertrophic chondrocytes seems to be reduced. When levels of PTH1R were analyzed in wt and nm E12 cartilage by semi-quantitative RT-PCR no significant differences in the expression levels were observed (Fig. 3B). As well, levels of the main ligand of PTH1R, PTHLH were also comparable in wt and nm E12 cartilage (Fig. 3B).

To determine whether the abnormal expression of IHH affects its function, we compared the expression of the hedgehog effector Patched (PTCH) in wt and nm E12 cartilage in serial sections probed with IHH, COL10A1 and FGFR3 (Fig. 4). As shown previously (compare Fig 2B and 3A) the normal largely non-overlapping pattern of COL10A1 and IHH is lost in the nm mutant. The expression of PTCH in wt GP is localized in a pattern similar to that described for proliferative and hypertrophic zones and in the perichondrium at the level of IHH expression in mammalian limbs (St-Jacques et al., 1999); PTCH expression in the nm limbs remains strong in the perichondrium at the level of the bone collar, but in the proliferative zone it is disorganized, irregular and narrow. Furthermore, the distance from the epiphyseal perichondrium to the PTCH domain is expanded in the nm GP, perhaps indicating alterations in the IHH gradient. Expression of FGFR3, which has been described as encompassing the proliferative and hypertrophic zones in the mammalian GP (Colvin et al., 1996), was found to be similar the wt chick GP. In the nm growth plate, as observed for PTCH expression, the distance from the epiphyseal perichondrium to the FGFR3 domain is expanded compared to wt (Fig. 4, see brackets).

To assess whether the observed changes in matrix and signaling molecule expression alter the extent of calcification in nm bone, von Kossa staining for calcium deposits and trabecular cytoarchitecture was performed on nm and wt E12 limbs. Normal, although somewhat more compacted, calcified trabeculae were observed in nm limbs, indicating that calcification proceeds normally in the absence of aggrecan (Supplemental Fig. 1).

Formation of the GP in the absence of aggrecan

Evaluation of the fully formed GP (E12) indicated significant morphological, molecular and signaling differences between wt and the aggrecan-deficient nm mutant (Fig. 1-4), but provided little mechanistic insight into how these aberrant phenotypes arise. To investigate the possibility that expression of COL10A1 and IHH in the E12 nm GP could be due to accelerated hypertrophy in the absence of aggrecan and to determine the progression of phenotypic and genotypic changes during limb development in the aggrecan-deficient mutants, the expression patterns of cartilage-specific markers were analyzed by *in situ* hybridization on serial sections from the E7-8 developmental interval, the critical period when hypertrophic chondrocytes first appear (Fig.5). In E7 (stage HH31) wt embryos, aggrecan was expressed strongly and fairly uniformly along the cartilage anlage (Fig. 5A). IHH expression was detected in the middle of the aggrecan expression domain and was clearly absent from distal portions of the cartilage elements (Fig. 5 C). Very faint expression of COL10A1 (Fig. 5 E), a marker of hypertrophic chondrocytes, was detectable in a few cells in the central region of the IHH expression domain, and OPN, a marker of late hypertrophic chondrocytes and osteoblasts, was barely detectable in the perichondrium surrounding the IHH-expressing domain in wt embryos (Fig.5 G arrow and inset). By E8 in wt embryos, aggrecan expression encompasses the entire element with an obvious diminution in the center, presumably representing initiation of the hypertrophic zone in each element. Strong aggrecan expression is detected distally as the two pre-hypertrophic domains begin to separate (Fig. 5 I), leading to the formation of dual proliferative and pre-hypertrophic zones. Note that the areas with the highest levels of aggrecan (AGC1) mRNA are coincident with IHH expression (Fig. 5 I, K), which remains true up to E12 (Fig. 3, 4). The IHH expression domain also splits into two regions by E8 (Fig. 5 K), each distal to the central expression domain of COL10A1 (Fig. 5 M). The expansion in length and width of the twin IHH domains is approximately three-fold in each dimension, reflecting the significant growth of the wt element during this 24 h period. The expression of OPN in E8 wt limbs is more distinct in the perichondrium and encompasses the entire length of the IHH-expressing domain (Fig. 5 O, arrow and inset).

In nm embryos at the very early stage (E7), there was a slight reduction in size of the skeletal elements but no other gross phenotypic differences compared to wt, although there was no expression of AGC1 mRNA (Fig. 5 B). The extent of the IHH-expression domain was comparable between wt and nm and IHH expression was somewhat reduced in intensity in the mutant (Fig. 5 C, D). Most surprisingly, expression of COL10A1 (Fig. 5 F) was strongly up-regulated, exhibiting a domain of mRNA expression that nearly overlapped the entire IHH region (Fig. 5 D), indicating precocious differentiation to the hypertrophic phenotype. At this early stage there was also moderate up-regulation of OPN expression localized to the perichondrium of nm cartilage elements, spanning the length of the IHH/COL10A1 domain, also suggesting accelerated hypertrophy and ossification (Fig. 5 H arrow and inset). At E8, the size of the nm cartilage element had begun to diminish (40% reduction) in width and length compared to wt. Also in contrast to wt, division of the IHH expression region into two distinct domains was not as evident as in the nm mutants by E8 (Fig. 5 L), and the overall expansion of the IHH-expression domains between E7 and E8 in nm embryos was less than 30% (Fig. 5 D, L). COL10A1 continued to exhibit a robust expression domain at E8 which still mostly overlapped that of IHH (Fig. 5 N), again indicating accelerated differentiation to hypertrophic chondrocytes in nm embryos. Furthermore, there was demonstrable GP maturation in nm E8 cartilage elements as evidenced by the significantly increased and nearly overlapping expression patterns of OPN and COL10A1 (Fig. 5 N, P arrow and insert). By E8, osteocalcin started to be detected in the periosteum and the levels were comparable between wt and nm GP (data not shown).

Since very limited information is available regarding expression of IHH and COL10A1 during the initial establishment of the GP, we attempted to distinguish between two possible mechanisms that could explain these early phenotypic changes in the aggrecan-null model using fluorescent *in situ* hybridization (FISH) of individual cells: i) whether normal chondrocytes that differentiate from the pre-hypertrophic to the hypertrophic state require down-regulation of IHH expression before up-regulation of COL10A1 can occur; or, ii) whether an intermediate zone is generated in which the same cells express both markers at the same time, making this process a transitional event rather than a switch from one stage to the next. We then asked whether this process is affected in the nm mutant. Confocal images of both E7 and E8 wt GP showed robust and restricted chondrocyte expression of IHH and COL10A1 (Fig. 6), and a very limited number of cells displaying co-expression (yellow cells). At E7, the nm IHH expression domain was only slightly smaller than in wt, but by E8 the IHH expression domain was significantly reduced in size (see also Fig. 5). As also shown in Fig. 5, COL10A1 expression in the mutant was strong at both E7 and E8, although the domain of expression did not grow. However, in contrast to wt, co-expression in the mutant GP, observed by confocal microscopy was extensive, to the extent that only a very small area expressed IHH exclusively (E8 wt and nm merge panels, brackets). Thus, it would appear that in normal GP development IHH expression is down-regulated prior to the up-regulation of COL10A1, allowing only a minimal number of cells to be in a transitional stage. Further, the ability of chondrocytes to down-regulate the expression of IHH during differentiation of pre-hypertrophic to hypertrophic, appears to be influenced by the presence or absence of an aggrecan-rich matrix.

Since reduced expression domains for IHH were observed in the nm mutant as early as E7 (Fig. 5, 6), we determined whether even earlier events, i.e. differentiation of chondroblasts to pre-hypertrophic chondrocytes in E6 embryos were affected by the lack of aggrecan expression by analyzing levels of IHH via whole mount *in situ* hybridization. This approach offers the advantage that the earliest stages of development are detectable, since limb differentiation occurs in a proximal-to-distal sequence and the distal condensations of the limb are at the least mature stages of differentiation. The area and apparent intensity of IHH expression in the ulna, radius and digits 2, 3 and 4 were similar between wt and nm at E6 (Fig. 7 A). Although patterns of IHH expression appear normal, potential differences in the IHH expression domains were quantified in two sets of ten independent embryos each using ImageJ software (Fig. 7 B), and overall IHH mRNA levels were assessed by semi-quantitative RT-PCR on wt and nm E6 RNA (Fig. 7 C). No significant differences were consistently observed by either approach, indicating that the initial temporal differentiation of chondroblasts to pre-hypertrophic chondrocytes is normal in the nm mutant.

To determine whether IHH signaling topography is affected in the early nm embryo, we monitored the expression of the hedgehog effector Patched (PTCH) in E6 limbs (Fig. 8). While expression of PTCH was observed in the developing wt perichondrium, the extent of PTCH expression in the mutant limb was broader, indicating an expanded area of initial IHH signaling when aggrecan is not being expressed in the cartilage element at this early stage of GP formation. Changes in BMP6 and FGFR3 expression were also evident at this early stage (Fig. 8). The pattern of BMP6 expression is similar in wt and nm limbs but it appears to be somewhat down-regulated in the mutant (Fig. 8). Interestingly, while FGFR3 is expressed all along the cartilage element and in the perichondrium at the level of the developing periosteum in E6 wt elements, expression of FGFR3 was already strongly down-regulated in the middle of the E6 nm element. Since FGFR3 has been implicated as a regulator of cell division during cartilage development (Ornitz and Marie, 2002), we analyzed cell division capacity in the early GPs of E6 embryos by BrdU incorporation. At this stage, cell division in the wt elements was seen to recede in the area where IHH expression was beginning (Fig. 9 A, C, E). Furthermore, in contrast to our results from the fully formed GP (E12), cell division in E6 epiphyseal cartilage

was down-regulated in the nm mutant qualitatively (Fig. 9 A, B) and quantitatively (Fig. 9 G); as well, the recession of the cell-division zone in the middle of the element was also accelerated (Fig. 9 B, F). Since these results could be indicative of de-regulation of FGF signaling, we biochemically analyzed one of the recognized down-stream indicators of FGF signaling in the GP, phosphorylated ERK (de Frutos et al., 2007). Western blot analysis of wt and nm E6 cartilage homogenates using an anti-phospho P42/44 MAPK antibody yielded a single 43 kDa band (Fig. 10A), as has been previously described for other chick tissues (Garcia et al., 2008). Quantification of phosphorylated ERK levels in E6 nm cartilage revealed an elevated level relative to that of wt cartilage (Fig. 10B).

Since our results thus far are indicative of de-regulation of both FGF and IHH signaling in the nm mutant, we investigated whether IHH signaling could modulate FGFR3 transcription using exogenous inhibition of IHH signaling in an organ explant culture system (Minina et al., 2002). We treated wt and nm E8 tibia explant cultures with cyclopamine over a 48h period and analyzed the resulting expression of COL10A1, IHH and FGFR3. An 11% and 7% reduction, respectively, in the length of wt and nm tibias in the presence of cyclopamine was observed concomitantly with higher expression of COL10A1 in both wt and nm limbs (Fig. 11). These observations are commensurate with the reported outcomes of similar mouse limb explant experiments (Minina et al., 2002). We also observed reduced FGFR3 expression domains in both wt and nm tibias when IHH signaling was inhibited (Fig. 11). Even though there is genetic evidence that FGFR3 regulates IHH expression (Colvin et al., 1996), these data indicate that the opposite is also possible.

TGF-beta and BMP signaling pathways

Since BMP6 and BMP2 have been implicated as negative regulators of hypertrophy (Yoon et al., 2006), we analyzed the activation of these pathways by determining levels of phospho-SMAD1/5/8 (P-SMAD1/5/8) in wt and nm GP. We also measured the levels of P-SMAD2, since other matrix-affected mutants such as the chondroitin-4 sulfotransferase-1 gene trap showed up-regulation of TGFβ signaling (Kluppel et al., 2005). Measurable levels of P-SMAD2 were not detected at E6, prior to the initiation of the maturation process (not shown). However, by E9, PSMAD2 immunoreactivity was observed throughout the whole skeletal element (Fig 12 A), and quantification of positive cells in the hypertrophic zone showed no statistical differences between the wt and nm GPs (Fig. 12 B). In contrast, P-SMAD1/5/8 was expressed preferentially in the hypertrophic zone (Fig. 12 A), and a significant increase in the number of positive cells was seen in the nm GP (Fig. 12B). These results may reflect a futile attempt by BMP signaling to slow down the maturation process in the nm mutant GP.

Gene expression in nm and wt chondrocyte cultures

To determine whether the defect in maturation of nm pre-hypertrophic chondrocytes is intrinsic to the chondrocytes or dependent on alteration of a signaling pathway regulated by the cytoarchitecture and matrix composition of the GP, we analyzed the maturation potential of nm chondrocytes in culture. A well-characterized primary culture model of spontaneous differentiation (Ferguson et al., 2000; Grimsrud et al., 1999; Iwamoto et al., 1993; Volk et al., 1998) established from E14 wt and nm sterna was used for this purpose. High levels of extracellular aggrecan were detected with the S103L antibody in wt cultures, while no extracellular expression of aggrecan in nm chondrocyte cultures was observed (Fig 13 A). As expected, wt cultures expressed high levels of both aggrecan and COL2A1 mRNA, while there was robust COL2A1 expression but minimal aggrecan expression in nm cell cultures (Fig. 13 B), paralleling the *in vivo* observations (Fig. 5) and indicating that nm chondrocytes are healthy and maintain normal morphology in culture. Fewer cells expressing COL10A1 and OPN mRNA, relative to the number of cells expressing COL2A1, were observed in both wt and nm cultures (Fig. 13 B); however, when the amounts of COL10A1 and OPN transcripts relative

to the levels of GAPDH mRNA in the cultures were measured to account for the total mass of cells (Fig. 13 C), nm chondrocytes appear not to be in an advanced state of differentiation as we described *in vivo* (Fig. 5). To determine whether this was due to increased cell division in the nm chondrocytes, BrdU incorporation and MTT assays were performed. Both a higher rate of cell division, as indicated by BrdU-positive incorporation (30% increase), and a greater number of cells, as reflected by increased MTT levels (40% increase), were observed in the nm cultures (Fig. 13 D).

To determine whether apoptotic pathways were also activated in the nm cultures as observed *in vivo*, analyses of caspase-3 and caspase-8 activities were performed. Activation of caspase-3 is a central event in the apoptotic process upon which numerous pathways converge, while caspase-8 activation is believed to be one of the initiation caspases at the beginning of the signaling cascade (Chen and Wang, 2002; Liu et al., 1996; Orth et al., 1996; Thornberry et al., 1997). In the nm cultures both activities were up-regulated approximately 2-fold with respect to the wt cultures, indicating increased prevalence of apoptosis in the nm culture (Fig. 13 E). Together, these data suggest that the nm cell proliferation capacity but not the differentiation potential is at least partially intrinsic to the chondrocyte.

DISCUSSION

Recently identified hereditary skeletal disorders associated with extracellular matrix gene mutations in humans and animal models are providing insights into the roles that the affected molecules play in skeletal development and growth (Schwartz, 2004). However, most of these studies have analyzed the fully developed mature GP of matrix-deficient models (Maddox et al., 1997; Savontaus et al., 1996; Wai et al., 1998; Watanabe and Yamada, 1999); therefore, little insight has been provided on the function of the matrix during GP formation or its influence on GP cell signaling. One recent study of a gene trap mutation in the chondroitin-4-sulfotransferase 1 (*C4st1*) gene which causes down-regulation of 4-O- sulfated chondroitin synthesis identified a severe chondrodysplasia that is characterized by strong up-regulation of TGFß signaling and down-regulation of BMP signaling (Kluppel et al., 2005). Furthermore, in the brachymorphic (bm) mouse, where levels of CS sulfation are reduced due a natural inactivating mutation of one of the isoforms of PAPS synthetase, PAPSS2 (Kurima et al., 1998), alterations in IHH signaling have been observed (Cortes M. et al, 2009), demonstrating that modification of the chondroitin sulfate component of aggrecan can adversely affect distinct signaling pathways during GP morphogenesis.

We have now obtained intriguing data from the avian aggrecan-deficient nm model, which revealed severe alterations in the genetic and developmental programs occurring in the nm GP concomitant with appearance of atypical morphology (Fig. 2-4). Strikingly, absence of aggrecan, the major proteoglycan component of cartilage matrix, is accompanied by dysregulation of several genes previously shown to be critical to the maturation process of hypertrophic chondrocytes and osteogenesis. First, although there appears to be both initiation and progression through the normal states of differentiation by nm chondrocytes (i.e., to expression of COL10A1), the hypertrophic zone is small and disorganized by the time a mature GP (E12) is formed. Secondly, based on the expression of a number of GP markers, the zones of pre-hypertrophic and hypertrophic cells that characterize a normal GP appear to overlap in the nm mutant (Fig. 1-3); a phenomenon which starts at the earliest stages of GP formation (E7) concomitant with the lack of aggrecan accumulation (Fig. 5-6). Thirdly, both *in vivo* and *in vitro*, lack of aggrecan in the ECM is associated with significant differences in numbers of cells in mutant versus wt GP caused by fluctuations in the proliferative and apoptotic pathways (Fig. 1 and 9), a phenomenon that also changes as GP maturation proceeds.

A role for IHH dysregulation underlying these changes in the nm GP was verified by analysis of PTCH expression in the mature growth plate which showed a narrow epiphyseal gradient in the nm mutant, suggesting that the lack of matrix could impair the normal IHH gradient (Fig. 4). The gene expression patterns of modulators critical to GP development in the E12 nm chick, in particular the overlapping expression of COL10A1, BMP6 and IHH mRNAs which obscures the normal distinctions between the pre-hypertrophic and hypertrophic regions, suggest acceleration of hypertrophy (Fig 2-4). Also, strong expression of OPN mRNA, a marker of late hypertrophic chondrocytes and osteoblasts, observed in a pattern that completely overlaps that of COL10A1 mRNA, suggests that acceleration of hypertrophy induces precocious bone formation in the nm mutant. Interestingly, advanced hypertrophy was already observed in the mutant when the hypertrophic chondrocytes are first detected in wt GP (E7-8) (Fig 5). Most importantly, IHH-expressing cells rapidly proceed to hypertrophy (expression of COL10A1) without down-regulating expression of IHH (Fig. 6), indicating loss of control of this critical switch. Consequently, i) the nm GP does not exhibit the characteristic pre-hypertrophic and hypertrophic zone demarcation; ii) separation and appositional growth of the twin GPs of each element is delayed; iii) vascular invasion becomes accelerated (up-regulation of OPN) and osteogenesis occurs prematurely; and iv) longitudinal as well as lateral growth is retarded.

Since the IHH-expressing domain is reduced from E7 onward, we tested whether this deficiency was driven by an even earlier (E6) abnormal setting of the IHH expression domain. Although, IHH appears to be turned on normally in the condensations (Fig. 7), arguing against precocious maturation of chondroblasts to pre-hypertrophic chondrocytes, the domain of expression of the hedgehog effector PTCH is broader in the perichondrium of the E6 nm elements, indicating a disturbance in the range of IHH signaling (Fig. 8) beyond the area where aggrecan is normally expressed, thus potentially modifying a key source of GP signaling, the developing periosteum. Several other important changes were observed in the aggrecan-deficient mutant at this critical period of early GP development. In contrast to the increased cell division observed during GP maturation in the nm mutant (E12), early stage (E6) nm epiphyseal cartilage exhibits a slightly lower rate of cell division. This cell division arrest observed in the area where IHH is expressed may be only slightly accelerated in the nm GP even though the levels of FGFR3, an important regulator of cell division and hypertrophic differentiation (Ornitz and Marie, 2002), are already strongly down-regulated in the forming pre-hypertrophic zone of the nm mutant (Fig. 8).

The changes observed in FGFR3 transcription levels and localization are difficult to explain since little is known about FGFR3 mRNA regulation in the developing GP. It is possible that the altered IHH signaling could elicit changes in FGF signaling, since our organ culture data (Fig 11) indicate changes in patterning and levels of FGFR3 expression when IHH signaling was inhibited by cyclopamine. Alternatively, is possible that early down-regulation of FGFR3 in the nm maturation zone might be an indicator of FGF signaling mis-regulation, as it has been reported that FGF-2 could down-regulate FGFR3 expression in culture (Ling et al., 2006). Both possibilities are supported by our finding that levels of phosphorylated ERK are up-regulated in E6 nm cartilage, as a result of either saturation of FGFR3 activation due to its down-regulation or alteration of FGF2 diffusion due to the lack of matrix. Thus, increased FGF signaling could explain the early down-regulation of cell division in the nm GP and the early depletion of FGFR3 in the nm pre-hypertrophic zone. This depletion of FGF signaling then could push IHH-expressing precursor cells to prematurely differentiate to hypertrophic chondrocytes, quickly depleting the pool of IHH-expressing cells and further driving cells into hypertrophy. Although only moderate reduction in BMP6 expression in the forming GP (E6) was observed, later (E9) increases in the level of BMP signaling in the hypertrophic zone was seen as determined by increased SMAD 1-5-8 phosphorylation (Fig 12); perhaps this occurs in response to the accelerated hypertrophy, since BMPs have been described as negative regulators of chondrocyte maturation (Minina et al., 2002;Minina et al., 2001). Increased BMP

signaling could be a reaction directed toward moderating the acceleration, or alternatively, simply a reflection of the accelerated terminal differentiation observed in the nm GP. Thereafter, the combined effects on the developing periosteum and continued down-regulation of FGFR3 ultimately could reduce FGF signaling, thereby accelerating cell division. It has been suggested that FGF and BMP signaling act in antagonistic and independent fashions upstream of IHH/parathyroid hormone-like protein signaling to define the zone where pre-hypertrophy will be initiated and also to regulate the rate of progression to hypertrophy. While FGF signaling is a negative regulator of cell division and suppresses hypertrophy, BMP signaling acts in parallel to IHH to induce proliferation and hinder hypertrophic differentiation (Minina et al., 2002). This last point has been contested in the literature since knock-outs of Bmpr1a in mouse suggest that BMP signaling is required for completion of terminal hypertrophic differentiation (Yoon et al., 2006). In the nm mutant, these three integrated signaling pathways appear to lose their balance-controlling influence after the initial IHH domain of expression is formed, possibly due to absence of a matrix in which to establish the respective gradient fields.

The lack of aggrecan in the nm matrix also may affect access by growth factors necessary for signaling between the perichondrium and the developing chondrocytes. Since part of the altered phenotype was retained in dispersed cell cultures, i.e. increased cell division and cell death, altered diffusion, or availability of signaling molecules in the nm mutant could be a factor. However, accelerated differentiation was not observed when the cytoarchitecture was destroyed by plating single cells from nm cartilage into culture, indicating that positional information and zonal signaling paradigms, as well as the integrity of the matrix and an intact perichondrium, are likely critically important to establishment of the hypertrophic phenotype (Fig. 12, 13). As well, we have not ruled out the contribution of changes caused by mechanical stresses due to muscle contraction in the developing limb; however, since clear modifications of signaling-molecule expression patterns are observed as early as E6, when limb size in the wt and nm are comparable, it is expected that these influences are secondary to the defects in GP formation.

Lastly, aggrecan-induced matrix deficiency may lead to premature and/or increased invasion of the nm GP hypertrophic region by blood vessels and osteoblasts; indeed, an anti-angiogenic function for the aggrecan matrix has been proposed (Fenwick et al., 1997). GP chondrocytes produce angiogenic factors (e.g., bFGF and VEGF) that recruit endothelial cells to migrate towards the hypertrophic cells (Carlevaro et al., 2000; Gerber et al., 1999), but this process may be altered in the absence of aggrecan, a known diffusion barrier to many factors in cartilage (Grodzinsky, 1983). The developmental expression pattern of aggrecan mRNA throughout the GP of normal limbs indicates that different states of chondrocyte differentiation require different levels of aggrecan in the extracellular matrix. The fact that pre-hypertrophic chondrocytes express the highest levels of aggrecan message in the wt GP is congruent with our finding in the nm mutant that the lack of aggrecan throughout the GP affects predominantly the transition of chondrocytes from the pre-hypertrophic to the hypertrophic phenotype. Also, the altered PTCH gradient in the nm limb suggests that aggrecan is essential for establishing a proper IHH gradient; these data are supported by the observations that IHH binds chondroitin sulfate chains *in vitro* and that in the undersulfated CSPG matrix of the bm mouse GP, a reduction in the extent of the IHH gradient has also been observed (Cortes M. et al. 2009). If IHH long range diffusion is impaired in matrix depleted of the major CSPG, aggrecan, such as in the nm limb, it may explain an increased PTCH signal towards the developing periostium at E6 and a reduced PTCH gradient in the fully formed GP (E12). Early changes in the IHH gradients could trigger changes in the other signaling pathways, or alternatively other ligand gradients could also be influenced by the altered matrix. In sum, our results indicate that an aggrecan-rich matrix is necessary for appropriate morphogen gradient formation; thereby indirectly modulating the coordination of several distinct signaling pathways during GP

morphogenesis. These findings take us a step closer to understanding the pathogenesis of chondrodysplasias, especially human disorders associated with mutations in the aggrecan gene (Gleghorn et al., 2005; Tompson et al., 2009).

Supplementary Material

Refer to Web version on PubMed Central for supplementary material.

Acknowledgments

We thank Dr. Edwin Ferguson and Dr. Leslie King for helpful discussion and Ms. Melissa Mueller and Antonia Navarro for excellent technical assistance. This work was supported by U.S. Public Health Service Grants HD-09402 and HD-17332.

REFERENCES

Amizuka N, Warshawsky H, Henderson JE, Goltzman D, Karaplis AC. Parathyroid hormone-related peptide-depleted mice show abnormal epiphyseal cartilage development and altered endochondral bone formation. J Cell Biol 1994;126:1611–23. [PubMed: 8089190]

Bruder SP, Caplan AI. Cellular and molecular events during embryonic bone development. Connect Tissue Res 1989;20:65–71. [PubMed: 2692958]

Brunner, T. Apoptosis Assay.. In: Spector, DL.; Goldman, RD.; Lieinwand, LA., editors. Cells: a laboratory manual. Vol. 1. Culture and Biochemical Analysis of Cells, Cold Spring Harbor Laboratory Press; New York: 1998. p. 15.15-15.17.

Carlevaro MF, Cermelli S, Cancedda R, Descalzi Cancedda F. Vascular endothelial growth factor (VEGF) in cartilage neovascularization and chondrocyte differentiation: autoparacrine role during endochondral bone formation. J Cell Sci 2000;113:59–69. [PubMed: 10591625]

Chen M, Wang J. Initiator caspases in apoptosis signaling pathways. Apoptosis 2002;7:313–9. [PubMed: 12101390]

Cohen MM Jr. Merging the old skeletal biology with the new. I. Intramembranous ossification, endochondral ossification, ectopic bone, secondary cartilage, and pathologic considerations. J Craniofac Genet Dev Biol 2000a;20:84–93. [PubMed: 11100738]

Cohen MM Jr. Merging the old skeletal biology with the new. II. Molecular aspects of bone formation and bone growth. J Craniofac Genet Dev Biol 2000b;20:94–106. [PubMed: 11100739]

Colvin JS, Bohne BA, Harding GW, McEwen DG, Ornitz DM. Skeletal overgrowth and deafness in mice lacking fibroblast growth factor receptor 3. Nat Genet 1996;12:390–7. [PubMed: 8630492]

Cortes M, Baria AT, Schwartz NB. Sulfation of chondroitin sulfate proteoglycans is necessary for proper Indian hedgehog signaling in the developing growth plate. Development 2009;136(10):1697–706. [PubMed: 19369399]

de Frutos CA, Vega S, Manzanares M, Flores JM, Huertas H, Martinez-Frias ML, Nieto MA. Snail1 is a transcriptional effector of FGFR3 signaling during chondrogenesis and achondroplasias. Dev Cell 2007;13:872–83. [PubMed: 18061568]

Domowicz MS, Sanders TA, Ragsdale CW, Schwartz NB. Aggrecan is expressed by embryonic brain glia and regulates astrocyte development. Developmental Biology 2008;315:114–124. [PubMed: 18207138]

Fenwick SA, Gregg PJ, Kumar S, Smith J, Rooney P. Intrinsic control of vascularization in developing cartilage rudiments. Int J Exp Pathol 1997;78:187–96. [PubMed: 9306926]

Ferguson CM, Schwarz EM, Reynolds PR, Puzas JE, Rosier RN, O'Keefe RJ. Smad2 and 3 mediate transforming growth factor-beta1-induced inhibition of chondrocyte maturation. Endocrinology 2000;141:4728–35. [PubMed: 11108288]

Garcia S, Lopez E, Lopez-Colome AM. Glutamate accelerates RPE cell proliferation through ERK1/2 activation via distinct receptor-specific mechanisms. J Cell Biochem 2008;104:377–90. [PubMed: 18022816]

Gerber HP, Vu TH, Ryan AM, Kowalski J, Werb Z, Ferrara N. VEGF couples hypertrophic cartilage remodeling, ossification and angiogenesis during endochondral bone formation. Nat Med 1999;5:623–8. [PubMed: 10371499]

Gleghorn L, Ramesar R, Beighton P, Wallis G. A mutation in the variable repeat region of the aggrecan gene (AGC1) causes a form of spondyloepiphyseal dysplasia associated with severe, premature osteoarthritis. Am J Hum Genet 2005;77:484–90. [PubMed: 16080123]

Grimsrud CD, Romano PR, D'Souza M, Puzas JE, Reynolds PR, Rosier RN, O'Keefe RJ. BMP-6 is an autocrine stimulator of chondrocyte differentiation. J Bone Miner Res 1999;14:475–82. [PubMed: 10234567]

Grodzinsky AJ. Electromechanical and physicochemical properties of connective tissue. Crit Rev Biomed Eng 1983;9:133–99. [PubMed: 6342940]

Hardingham TE, Muir H. Binding of oligosaccharides of hyaluronic acid to proteoglycan. Biochem. J 1973;135:905–908. [PubMed: 4273187]

Horton, WA. Morphology of Connective tissue: Cartilage.. In: Royce, PM.; Steinmann, B., editors. Connective Tissue and its Heritable Disorders: Molecular, genetic and medical aspects. Wiley-Liss, Inc; New York: 1993. p. 73-101.

Horton WE Jr. Feng L, Adams C. Chondrocyte apoptosis in development, aging and disease. Matrix Biol 1998;17:107–15. [PubMed: 9694591]

Incardona JP, Gaffield W, Kapur RP, Roelink H. The teratogenic Veratrum alkaloid cyclopamine inhibits sonic hedgehod signal transduction. Development 1998;125:3553–62. [PubMed: 9716521]

Iwamoto M, Golden EB, Adams SL, Noji S, Pacifici M. Responsiveness to retinoic acid changes during chondrocyte maturation. Exp Cell Res 1993;205:213–24. [PubMed: 8387013]

Karsenty G. The complexities of skeletal biology. Nature 2003;423:316–8. [PubMed: 12748648]

Kimata K, Oike Y, Tani K, Shinomura T, Yamagata M. A large chondroitin sulfate proteoglyan (PG-M) synthesized before chondrogenesis in the limb bud of chick embryo. J. Biol. Chem 1986;261:13517–13525. [PubMed: 3759975]

Kluppel M, Wight TN, Chan C, Hinek A, Wrana JL. Maintenance of chondroitin sulfation balance by chondroitin-4-sulfotransferase 1 is required for chondrocyte development and growth factor signaling during cartilage morphogenesis. Development 2005;132:3989–4003. [PubMed: 16079159]

Knudson CB, Knudson W. Cartilage proteoglycans. Semin Cell Dev Biol 2001;12:69–78. [PubMed: 11292372]

Kurima K, Warman ML, Krishnan S, Domowicz M, Krueger RC Jr. Deyrup A, Schwartz NB. A member of a family of sulfate-activating enzymes causes murine brachymorphism. Proc Natl Acad Sci U S A 1998;95:8681–5. [PubMed: 9671738]

Lee K, Deeds JD, Segre GV. Expression of parathyroid hormone-related peptide and its receptor messenger ribonucleic acids during fetal development of rats. Endocrinology 1995;136:453–63. [PubMed: 7835276]

Li H, Schwartz NB, Vertel BM. cDNA cloning of chick cartilage chondroitin sulfate (aggrecan) core protein and identification of a stop codon in the aggrecan gene associated with the chondrodystrophy, nanomelia. J Biol Chem 1993;268:23504–23511. [PubMed: 8226878]

Ling L, Murali S, Dombrowski C, Haupt LM, Stein GS, van Wijnen AJ, Nurcombe V, Cool SM. Sulfated glycosaminoglycans mediate the effects of FGF2 on the osteogenic potential of rat calvarial osteoprogenitor cells. J Cell Physiol 2006;209:811–25. [PubMed: 16972247]

Liu X, Kim CN, Yang J, Jemmerson R, Wang X. Induction of apoptotic program in cell-free extracts: requirement for dATP and cytochrome c. Cell 1996;86:147–57. [PubMed: 8689682]

Maddox BK, Garofalo S, Keene DR, Smith C, Horton WA. Type II collagen pro-alpha-chains containing a Gly574Ser mutation are not incorporated into the cartilage matrix of transgenic mice. Matrix Biol 1997;16:93–103. [PubMed: 9314159]

Minina E, Kreschel C, Naski MC, Ornitz DM, Vortkamp A. Interaction of FGF, Ihh/Pthlh, and BMP signaling integrates chondrocyte proliferation and hypertrophic differentiation. Dev Cell 2002;3:439–49. [PubMed: 12361605]

Minina E, Wenzel HM, Kreschel C, Karp S, Gaffield W, McMahon AP, Vortkamp A. BMP and Ihh/PTHrP signaling interact to coordinate chondrocyte proliferation and differentiation. Development 2001;128:4523–34. [PubMed: 11714677]

Mok SS, Masuda K, Hauselmann HJ, Aydelotte MB, Thonar EJ. Aggrecan synthesized by mature bovine chondrocytes suspended in alginate. Identification of two distinct metabolic matrix pools. J Biol Chem 1994;269:33021–7. [PubMed: 7806530]

Olsen BR, Reginato AM, Wang W. Bone development. Annu Rev Cell Dev Biol 2000;16:191–220. [PubMed: 11031235]

Ornitz DM, Marie PJ. FGF signaling pathways in endochondral and intramembranous bone development and human genetic disease. Genes Dev 2002;16:1446–65. [PubMed: 12080084]

Orth K, O'Rourke K, Salvesen GS, Dixit VM. Molecular ordering of apoptotic mammalian CED-3/ICE-like proteases. J Biol Chem 1996;271:20977–80. [PubMed: 8702858]

Quinn TM, Morel V, Meister JJ. Static compression of articular cartilage can reduce solute diffusivity and partitioning: implications for the chondrocyte biological response. J Biomech 2001;34:1463–9. [PubMed: 11672721]

Rose TM, Schultz ER, Henikoff JG, Pietrokovski S, McCallum CM, Henikoff S. Consensus-degenerate hybrid oligonucleotide primers for amplification of distantly related sequences. Nucleic Acids Res 1998;26:1628–35. [PubMed: 9512532]

Sandell LJ, Morris N, Robbins JR, Goldring MB. Alternatively spliced type II procollagen mRNAs define distinct populations of cells during vertebral development: differential expression of the amino-propeptide. J Cell Biol 1991;114:1307–19. [PubMed: 1894696]

Sandell LJ, Sugai JV, Trippel SB. Expression of collagens I, II, X, and XI and aggrecan mRNAs by bovine growth plate chondrocytes in situ. J Orthop Res 1994;12:1–14. [PubMed: 8113931]

Savontaus M, Vuorio E, Metsaranta M. Growth retardation in transgenic mice harboring a type II collagen mutation. Ann N Y Acad Sci 1996;785:328–30. [PubMed: 8702170]

Schwartz, NB. PAPS synthetase.. In: J. W. a. Sons. , editor. Encyclopedia of Mol. Med. Vol. 1. New York: 2002. p. 284-287.

Schwartz NB. Chondrodysplasias. Encyclopedia of Endocrine Disorders 2004;1:502–509.

Schwartz NB, Domowicz M. Chondrodysplasias due to proteoglycan defects. Glycobiology 2002a; 12:57R–68R.

Schwartz, NB.; Domowicz, MS. Proteoglycan gene mutations and impaired skeletal development.. In: Buckwalter, JA.; Ehrlich, MG.; Sandell, LJ.; Trippel, SB., editors. Skeletal Growth and Development. American Association of Orthopedic Surgeon Publications; Rosemont, IL: 1998. p. 413-433.

Schwartz NB, Domowicz MS. Chondrodysplasias due to proteoglycan defects. Glycobiology 2002b; 12:57R–68R.

Schwartz, NB.; Domowicz, MS. Encyclopedia of Endocrine Diseases. Vol. 1. Elsevier Inc.; San Diego, CA: 2004. Chondrodysplasias.; p. 502-509.

Schwartz, NB.; Hennig, AK.; Krueger, RC.; Krzystolik, M.; Li, H.; Mangoura, D. Developmental expression of S103L cross-reacting proteoglycans in embryonic chick.. In: Fallon, JF.; Goetinck, PF.; Kelley, RO.; Stocum, DL., editors. Limb Development and Regeneration. Wiley-Liss, Inc.; New York: 1993. p. 505-514.

Shibata S, Fukada K, Imai H, Abe T, Yamashita Y. In situ hybridization and immunohistochemistry of versican, aggrecan and link protein, and histochemistry of hyaluronan in the developing mouse limb bud cartilage. J Anat 2003;203:425–32. [PubMed: 14620382]

Solloway MJ, Dudley AT, Bikoff EK, Lyons KM, Hogan BL, Robertson EJ. Mice lacking Bmp6 function. Dev Genet 1998;22:321–39. [PubMed: 9664685]

St-Jacques B, Hammerschmidt M, McMahon AP. Indian hedgehog signaling regulates proliferation and differentiation of chondrocytes and is essential for bone formation. Genes Dev 1999;13:2072–86. [PubMed: 10465785]

Thompson, S.; Hunt, R. Histochemical procedures: von Kossa staining for calcium.. In: Thomas, editor. Selected histochemical and histophatological methods. Vol. IL. Springfield: 1966. p. 582-584.

Thornberry NA, Rano TA, Peterson EP, Rasper DM, Timkey T, Garcia-Calvo M, Houtzager VM, Nordstrom PA, Roy S, Vaillancourt JP, Chapman KT, Nicholson DW. A combinatorial approach defines specificities of members of the caspase family and granzyme B. Functional relationships established for key mediators of apoptosis. J Biol Chem 1997;272:17907–11. [PubMed: 9218414]

Tompson SW, Merriman B, Funari VA, Fresquet M, Lachman RS, Rimoin DL, Nelson SF, Briggs MD, Cohn DH, Krakow D. A recessive skeletal dysplasia, SEMD aggrecan type, results from a missense

mutation affecting the C-type lectin domain of aggrecan. Am J Hum Genet 2009;84:72–9. [PubMed: 19110214]

Volk SW, Luvalle P, Leask T, Leboy PS. A BMP responsive transcriptional region in the chicken type X collagen gene. J Bone Miner Res 1998;13:1521–9. [PubMed: 9783540]

Vortkamp A, Lee K, Lanske B, Segre GV, Kronenberg HM, Tabin CJ. Regulation of rate of cartilage differentiation by Indian hedgehog and PTH-related protein. Science 1996;273:613–22. [PubMed: 8662546]

Wagner EF, Karsenty G. Genetic control of skeletal development. Curr Opin Genet Dev 2001;11:527–32. [PubMed: 11532394]

Wai AW, Ng LJ, Watanabe H, Yamada Y, Tam PP, Cheah KS. Disrupted expression of matrix genes in the growth plate of the mouse cartilage matrix deficiency (cmd) mutant. Developmental Genetics 1998;22:349–58. [PubMed: 9664687]

Watanabe H, Yamada Y. Mice lacking link protein develop dwarfism and craniofacial abnormalities. Nat Genet 1999;21:150–1. [PubMed: 9988260]

Wight, TN.; Heinegard, DK.; Hascall, VC. Proteoglycans, Structure and Function. Plenum Press; New York: 1991.

Yoon BS, Pogue R, Ovchinnikov DA, Yoshii I, Mishina Y, Behringer RR, Lyons KM. BMPs regulate multiple aspects of growth-plate chondrogenesis through opposing actions on FGF pathways. Development 2006;133:4667–78. [PubMed: 17065231]

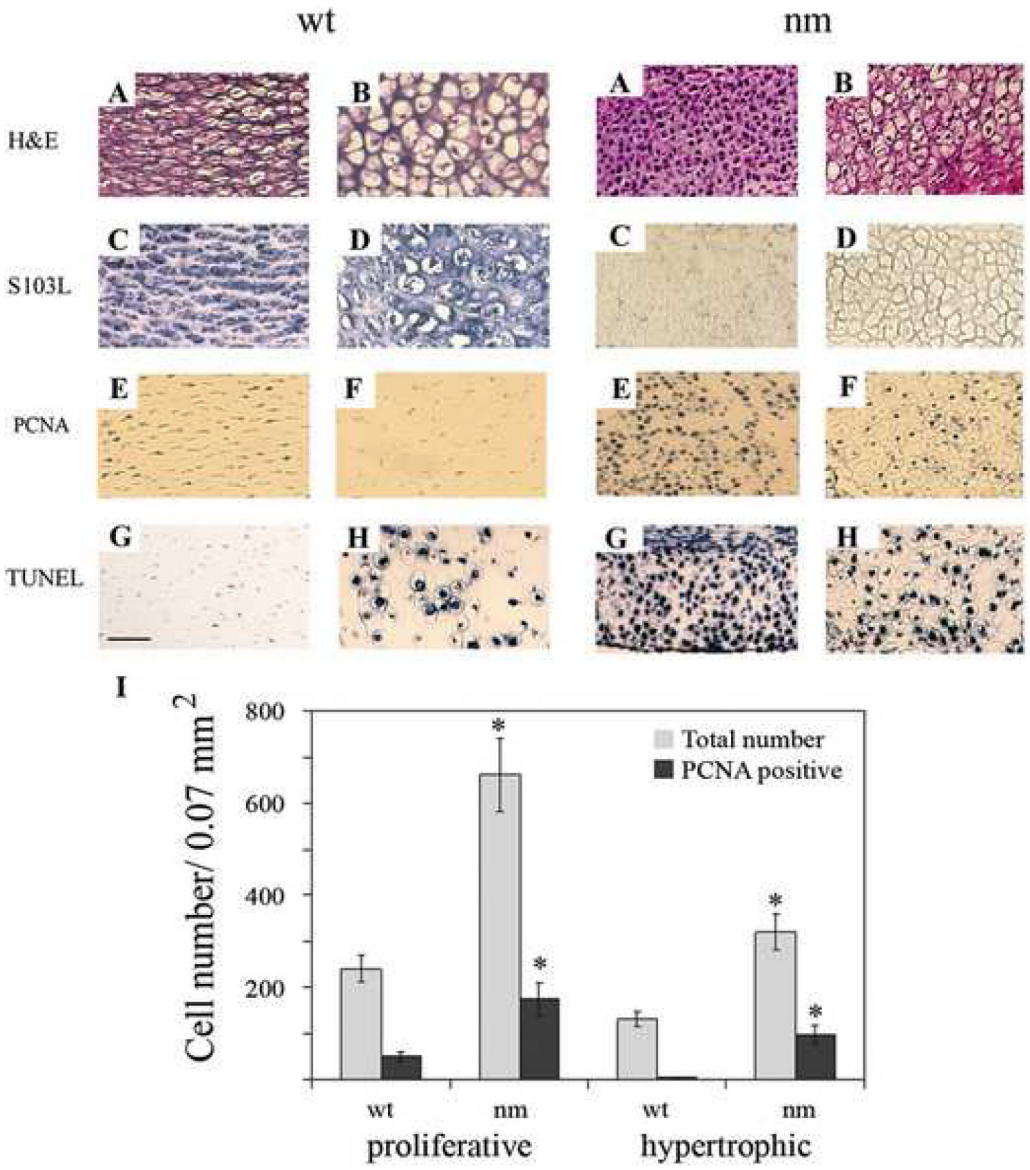

Figure 1. Patterns of cell death and proliferation in wild type (wt) and nanomelic (nm) embryos

Images depict proliferative (A,C,E,G) and hypertrophic (B, D, F, H) chondrocyte zones from E12 wt and nm tibial limb sections. Paraffin sections were stained with hematoxylin-eosin (A, B) and immunostained with S103L antibody (C, D). Proliferative cells were detected with anti-PCNA antibody (E, F) and apoptotic cells were detected by TUNEL staining (G, H). Scale bar: 50 μm. I. **Chondrocyte proliferation in wt and nm E12 limbs.** Average numbers of PCNA-positive cells per field were determined by immunocytochemistry and total numbers of cells from phase-contrast photographs of the same fields. A total of 6-8 0.07 mm^2 fields each from wt and nm proliferative and hypertrophic zones were counted. * $p<0.0001$

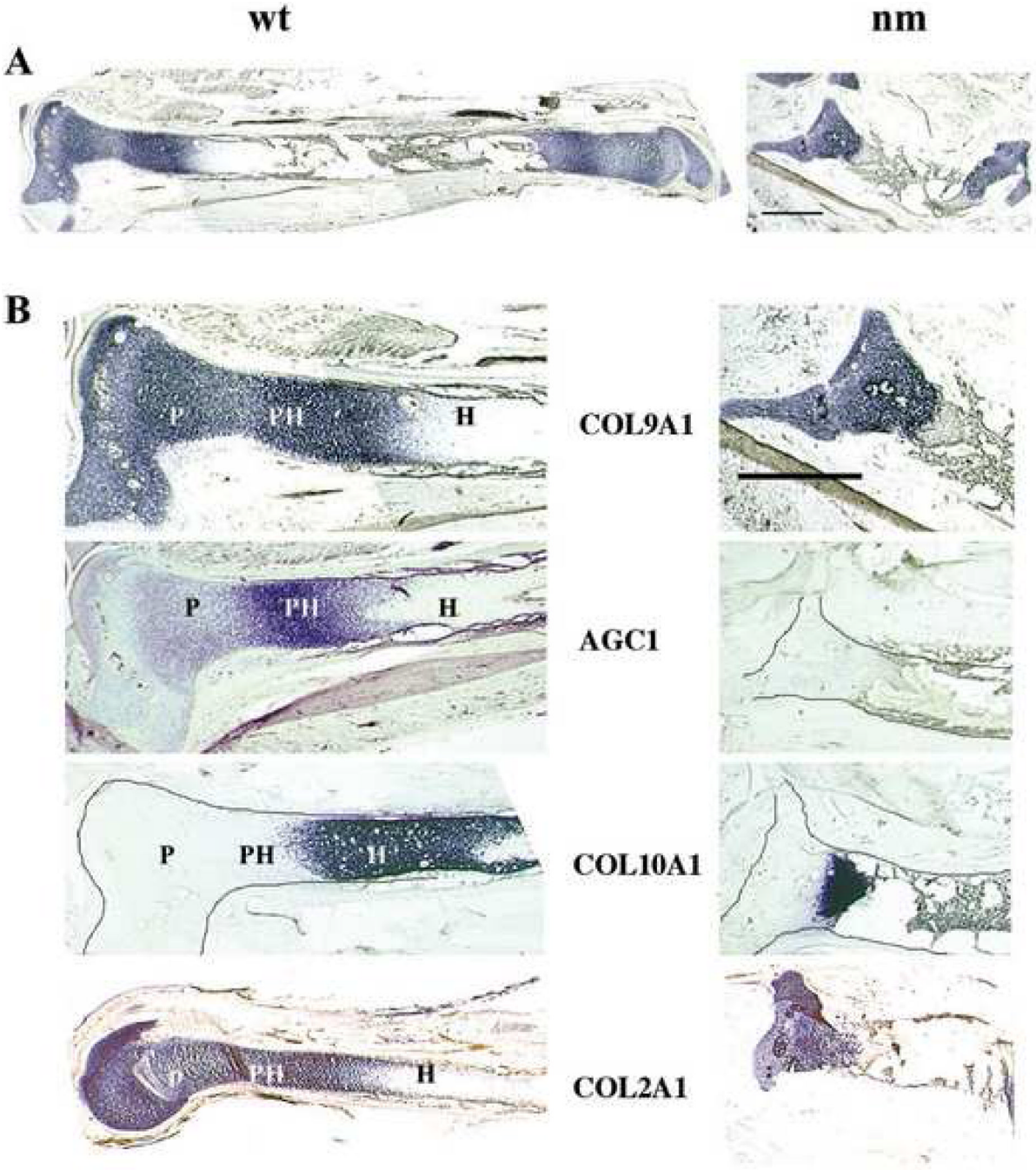

Figure 2. Expression of matrix protein genes

A. Expression of collagen type IX (COL9A1) in E12 tibia sections from wt and nm chicks detected by *in situ* hybridization. Three sections from each of 10 embryos were analyzed with consistent results. **B.** Higher magnification of E12 limb sections hybridized with probes for collagen type IX (COL9A1), aggrecan (AGC1), collagen type X (COL10A1), and collagen type II (COL 2A1). *In situ* hybridizations with DIG-labeled probes were performed on 40 μm tibia sections. When necessary, cartilage element limits were outlined. P: proliferative zone; PH pre-hypertrophic zone; H: hypertrophic zone. Scale bar: 1mm.

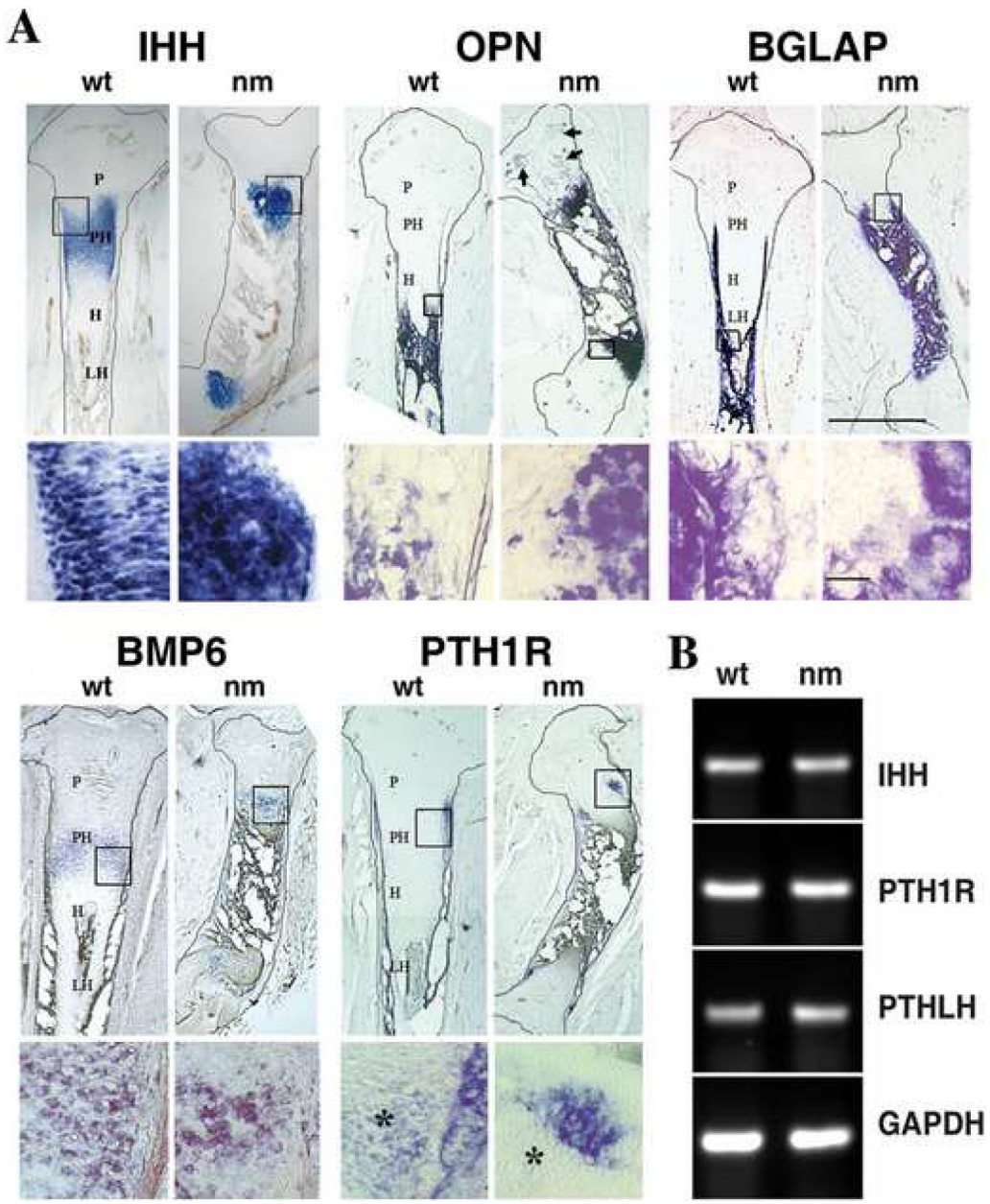

Figure 3. Expression profiles of regulatory genes

A. Upper images in each group: expression of Indian hedgehog (IHH), bone morphogenic protein 6 (BMP6), PTHrP receptor (PTH1R), osteopontin (OPN) and osteocalcin (BGLAP) detected by *in situ* hybridizations using DIG-labeled probes in 40 μm tibia sections from wt and nm E12 embryos. Scale bar: 1mm. Each lower row image shows a higher magnification of the boxed area in the respective upper row photograph. Asterisks (*) indicate chondrocyte expression of PTH1R. Arrows indicate secondary ossification sites in nm GP. PH: pre-hypertrophic zone; H: hypertrophic zone. LH: late hypertrophic zone. Scale bar: 150 μm. **B.** Semi-quantitative RT-PCRs for IHH, PTH1R and parathyroid hormone-related peptide (PTHLH) performed on wt and nm E12 cartilage RNA.

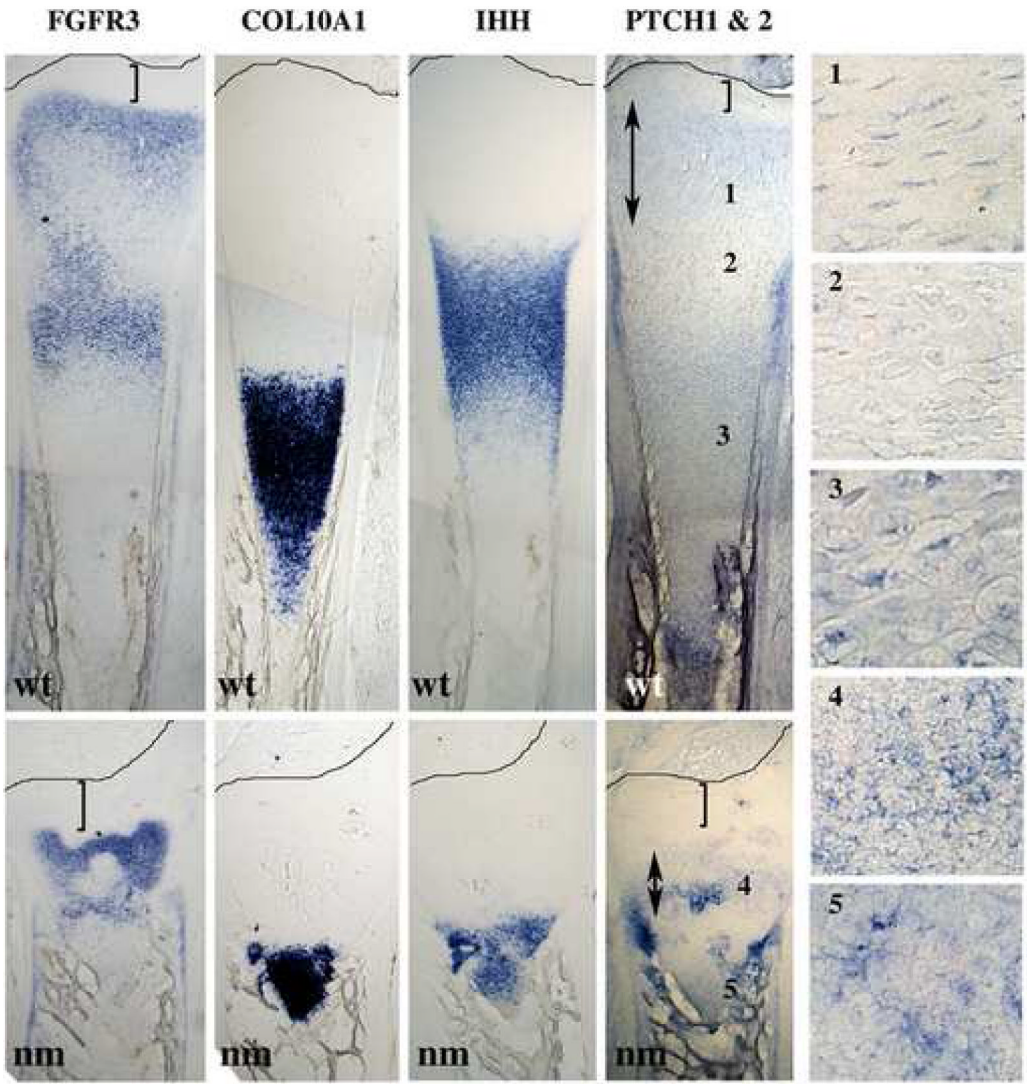

Figure 4. Comparative expression profiles

Expression of FGFR3, COL10A1, IHH, and PTCH (1&2) mRNAs, detected by *in situ* hybridizations using DIG-labeled probes in serial 40 μm tibia sections from wt and nm E12 embryos. Numbered insets are close-ups of the areas indicated in the PTCH expression panel. Double arrows indicate the extent of the epiphyseal expression of PTCH. Brackets indicate the distance between the epiphyseal domain of expression and the perichondrium. Lines mark the perichondrium boundaries.

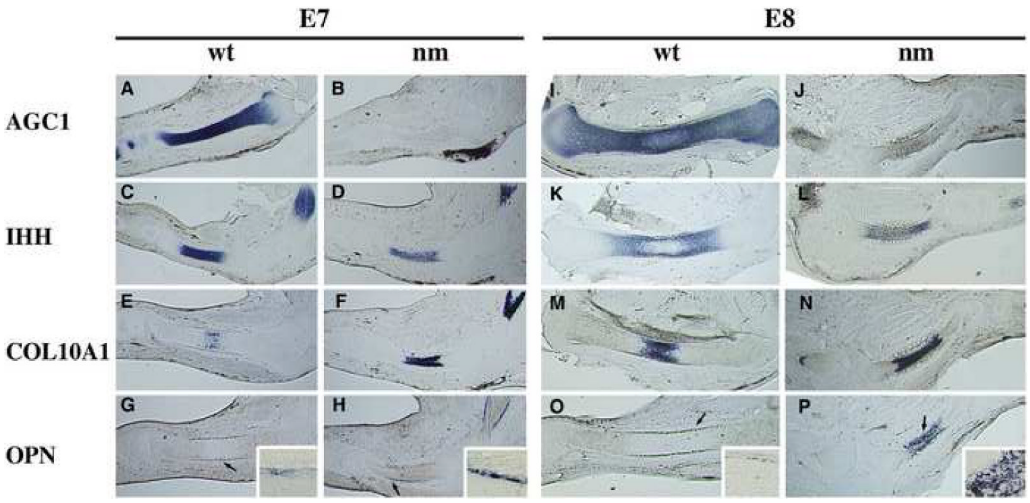

Figure 5. Establishment of a GP without aggrecan

Expression patterns of aggrecan (AGC1) (A, B, I, J), Indian hedgehog (IHH) (C, D, K, L), collagen type X (COL10A1) (E, F, M, N) and osteopontin (OPN) (G, H, O, P) in E7 (A-H) and E8 (I-P) limb sections from wild-type (wt) (A-C, E, G; I, K, M, O) and nanomelic (nm) (B, D, F, H; J, L, N, P) chicks. *In situ* hybridizations with gene-specific DIG-labeled RNA probes were performed on 40 μm sections. Arrows designate areas enlarged in corner insets of G, H, O and P.

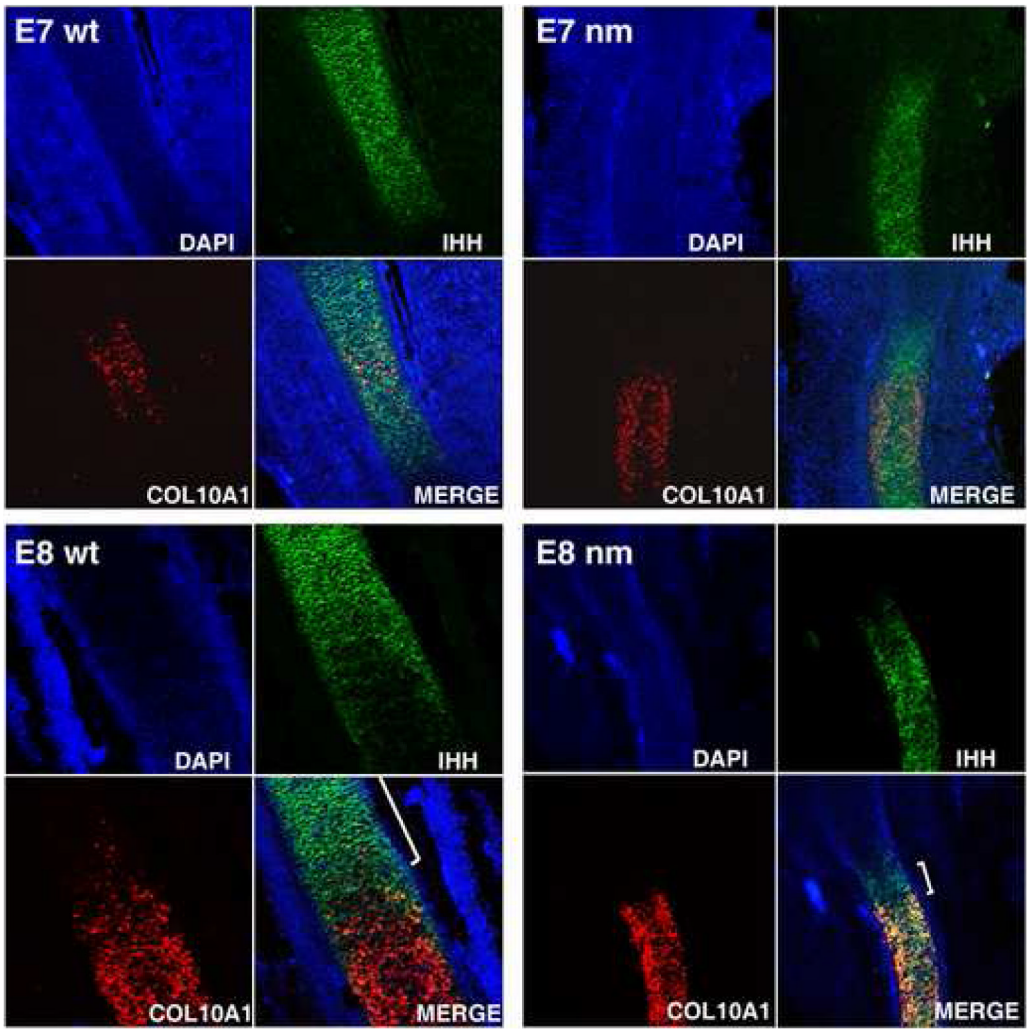

Figure 6. Maturation of the nm GP

DAPI-counterstained, Indian hedgehog (IHH) and collagen X (COL10A1) gene expression and merged composite images , from E7 and E8 nm and wt tibia sections. Fluorescent *in situ* hybridizations (FISH) with gene-specific DIG-labeled RNA probes were performed on 40 μm sections. The IHH and COL10A1 co-expression area is temporally enhanced in the nanomelic (nm) growth plate while the area expressing exclusively IHH is reduced in the E8 nm GP (white brackets in the E8 merge images).

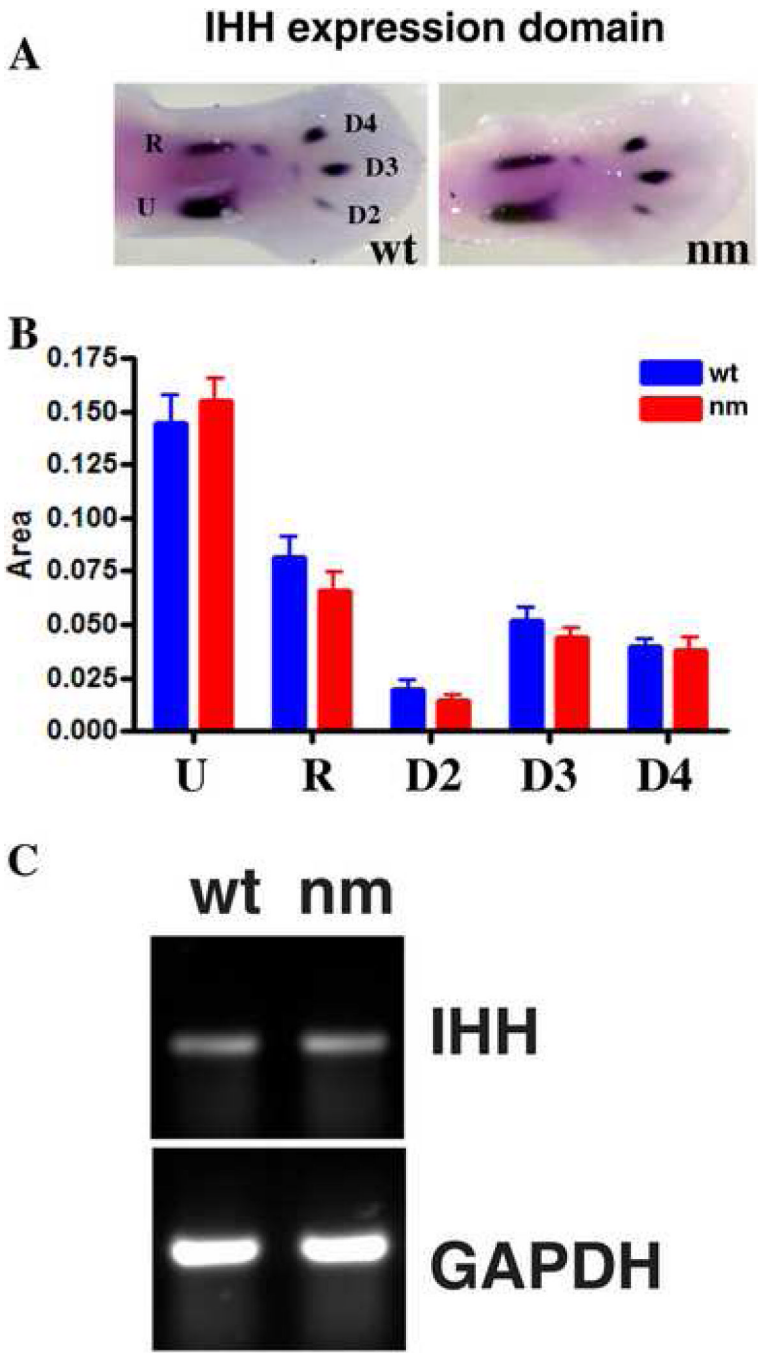

Figure 7. Initiation of hypertrophy in nanomelic GP

A. Expression of IHH in E6 wt and nm limbs visualized by whole mount *in situ* hybridizations. **B.** The areas of IHH expression were quantified for the ulna (U), radius (R) and digits 2 (D2), 3 (D3), and 4 (D4) in 10 limbs each from nm and wt embryos using the NIH ImageJ software package. **C.** Consistent levels of IHH were observed in E6 limbs RNA by semi-quantitative RT-PCR.

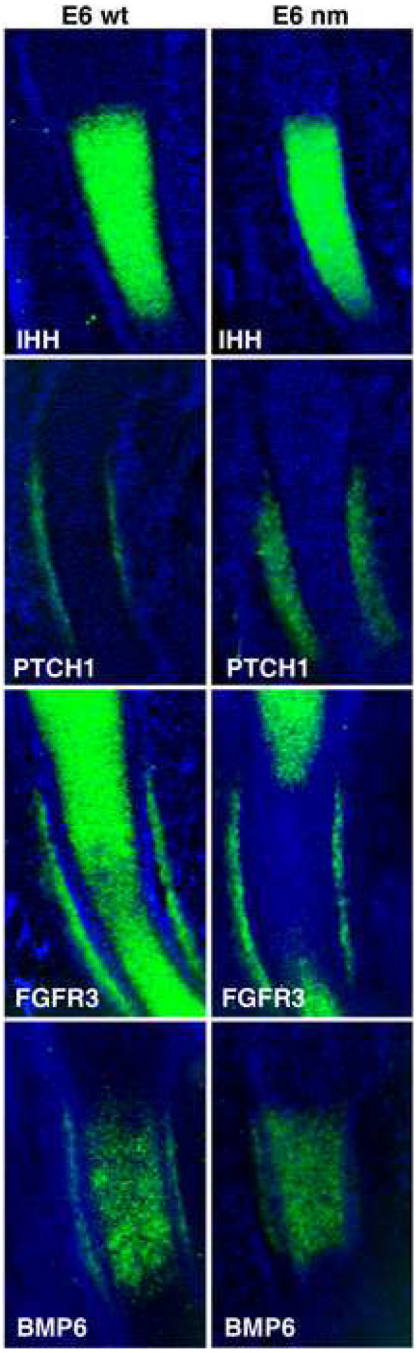

Figure 8. Nanomelic growth plate at E6

Expression patterns of IHH, PTCH1, FGFR3, and BMP6 in E6 limb sections from wt and nm chick embryos. The mRNAs were detected by in situ hybridization with DIG-labeled RNA probes (signal was assigned the pseudo-color green). Sections were counterstained with DAPI.

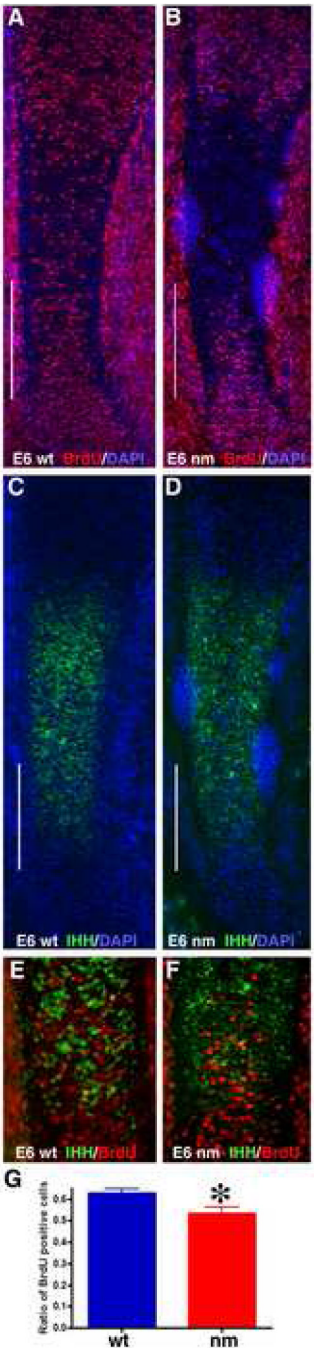

Figure 9. Early decreased cell division in pre-hypertrophic chondrocytes

After 3 h of BrdU incorporation (1.6 mg/100μl), dividing cells were visualized in tibia sections from wt and nm (A, B, red) E6 embryos after IHH mRNA was detected by FISH (C, D, green). Sections were counterstained with DAPI. White lines indicate the areas enlarged in the merged images (E, F). Numbers of BrdU-positive cells were quantified in ten comparable but independent areas from both wt and nm embryos (G). Data was evaluated for statistical significance using the Student's *t*-test. *<0.008

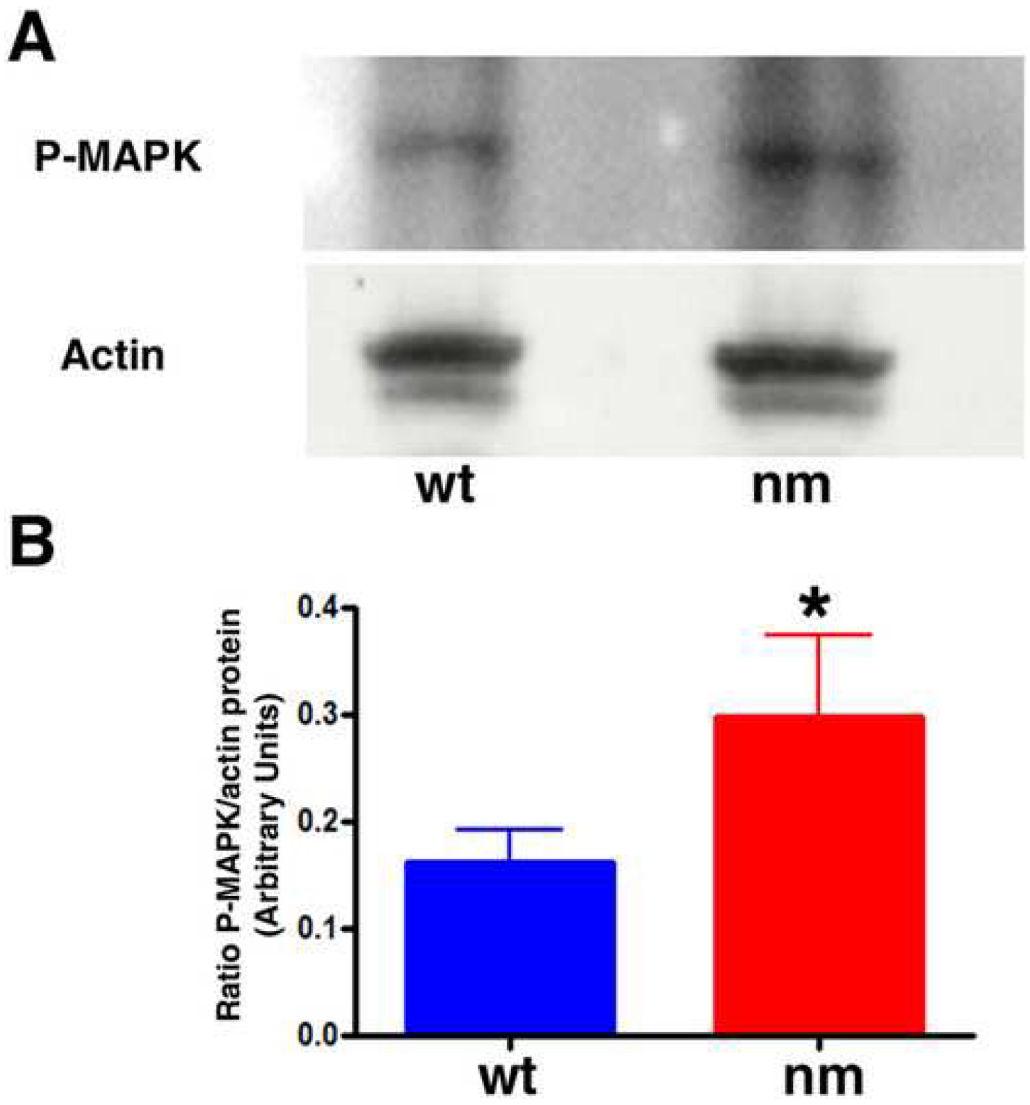

Figure 10. Phosphorylated MAPK is increased in E6 nm cartilage

A. Immunobloting analysis showing levels of phosphorylated MAPK (Erk), and β-actin as a loading control, in E6 wt and nm cartilage lysates. **B.** Relative levels of phosphorylated MAPK to β-actin were quantified in three independent experiments. Data was evaluated for statistical significance using the Student's *t*-test. *< 0.04.

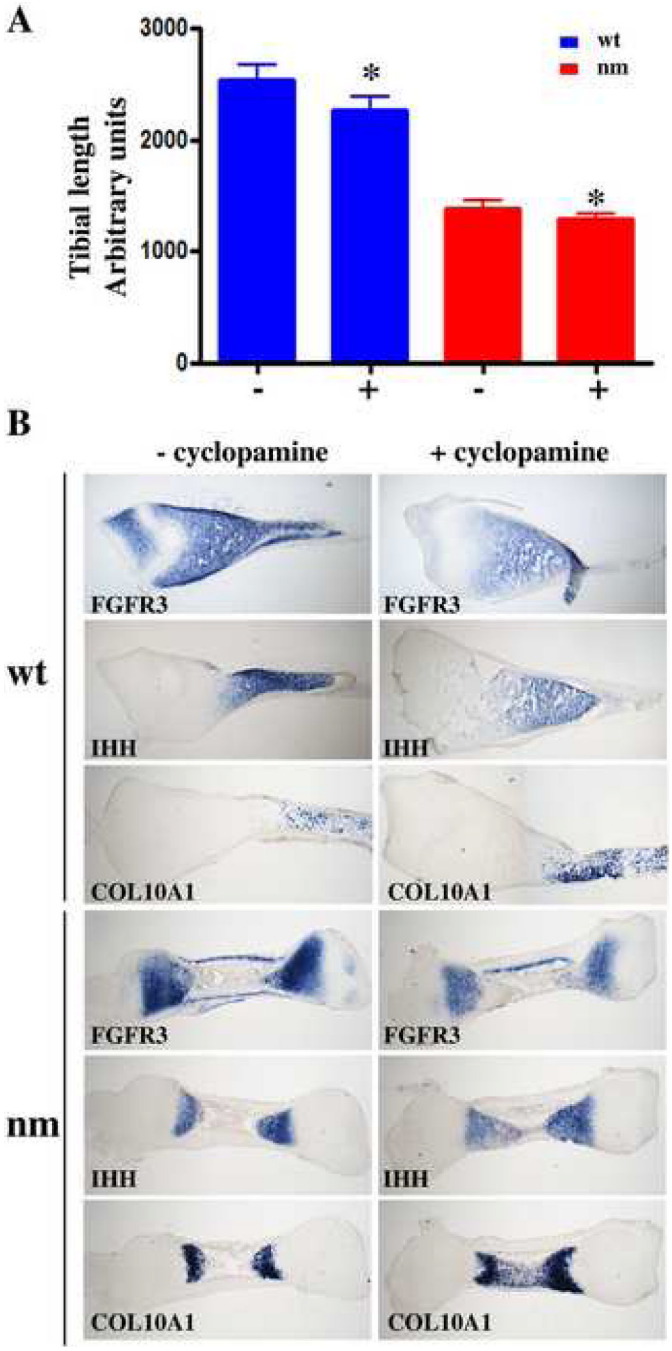

Figure 11. Interaction of IHH and FGF signaling

Matched wt and nm E8 tibias were cultured for 2 days with (+) or without (−)10μM cyclopamine. **A.** Total tibial length at the end of the culture time was measured using the ImageJ program, and data were evaluated for statistical significance using the Student's *t*-test for correlated samples. * $p<0.001$. **B.** Expression of FGFR3, IHH, and COL10A1 detected by *in situ* hybridizations using DIG-labeled probes in serial 40 μm sections from wt and nm cultured tibia explants with or without cyclopamine treatment.

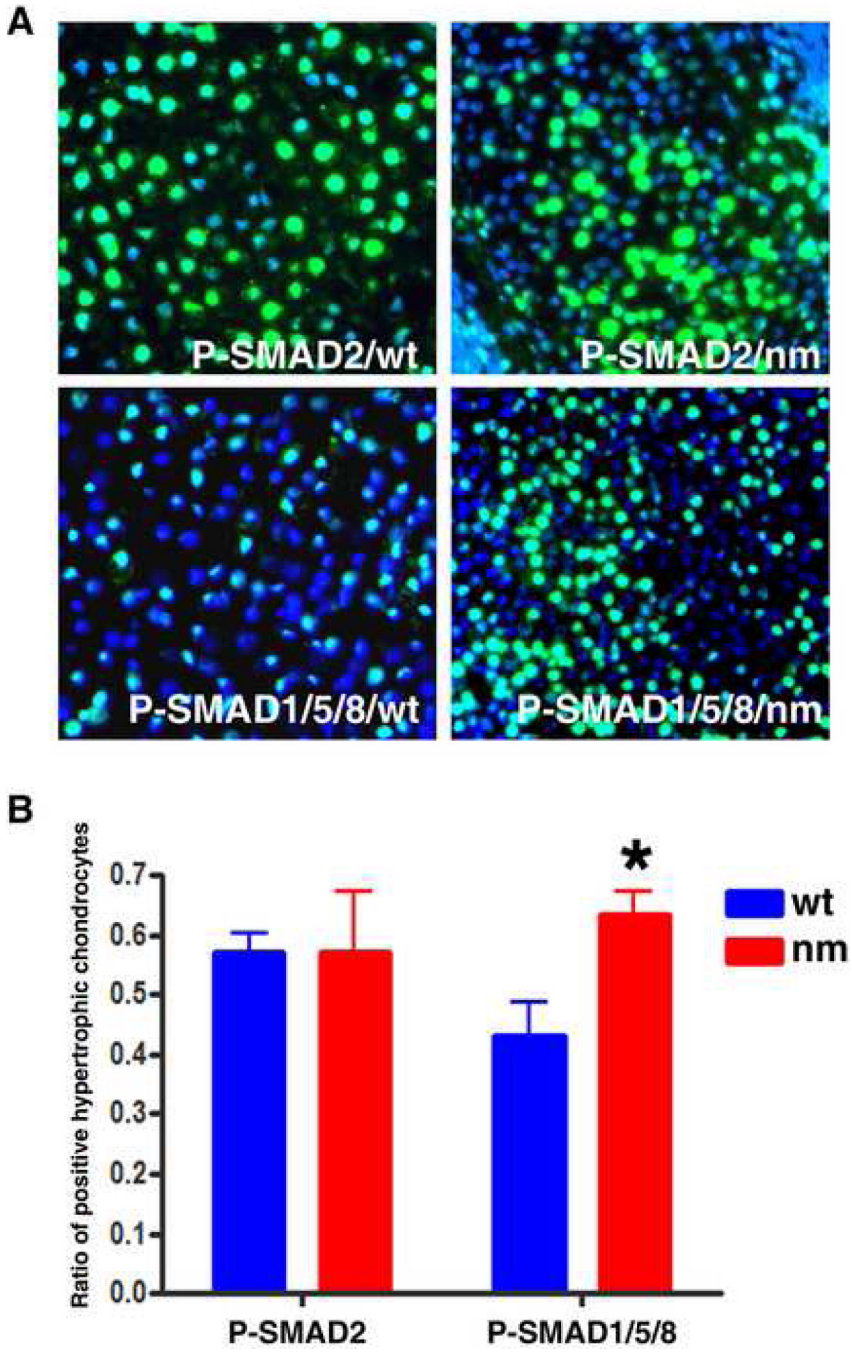

Figure 12. Hypertrophic chondrocytes expressing P-SMAD1/5/8 are increased in nm GP compared to wt

A. Immunocytochemical staining with P-SMAD 2 and P-SMAD1/5/8 specific antibodies showed comparable levels of P-SMAD2 and increased levels of P-SMAD1/5/8 in hypertrophic chondrocytes of E9 nm GP with respect to wt. Sections were counterstained with DAPI. **B.** The numbers of P-SMAD2- and P-SMAD1/5/8- positive cells relative to total numbers of cells (DAPI-positive nuclei) in seven independent fields each from wt and nm limbs were determined using ImageJ software. Data was analyzed for statistical significance using the Student's *t*-test.

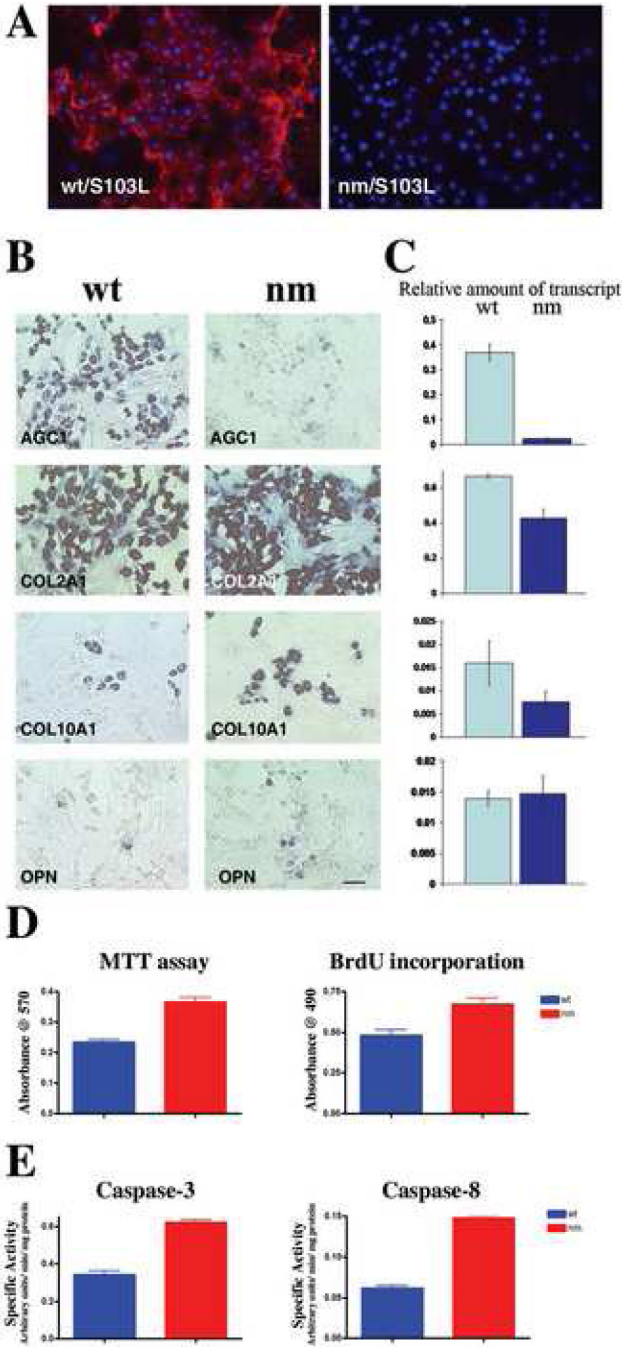

Figure 13. Expression of matrix component genes by wt and nm chondrocytes in culture

A. Wt and nm chondrocyte cultures immunostained with S103L antibody (red) without permeabilization, so as to detect only extracellular aggrecan. **B.** Expression of AGG, COL2A1, COL10A1 and OPN messages detected by *in situ* hybridization in cultured chondrocytes from wt and nm E14 sterna. Scale bar 35μm. **C.** The bar graphs show levels of AGC1, COL2A1, COL10A1 and OPN transcripts relative to levels of GAPDH mRNA in wt and nm chondrocyte cultures. Quantification was performed using the same *in situ* hybridization protocol but replacing the NBT/BCIP substrate of alkaline phosphatase with the fluorescent substrate MUP. Determinations were performed on triplicate wells for each probe sample. Bars represent standard deviations. **D.** Cell-proliferation in cultured wt and nm chondrocytes. Cell viability

was determined by assessing mitochondrial activity using the MTT assay and cell proliferation measured by determining 4-hour BrdU-incorporation levels for chondrocytes from wt and nm E14 sterna maintained in culture for 6 days. **E.** Apoptotic pathways in cultured wt and nm chondrocytes. Activation of the apoptotic pathway was assessed by determining the specific activities of caspase-3 and caspase-8 using the fluorogenic substrates Ac-DEVD-AFC and Ac-IETD-AFC, respectively. The results are shown as the mean ± SD(bars), $p<0.005$ for the MTT and proliferation assays and $p<0.001$ for both caspase assays. In all the experiments dissociated chondrocytes were culture for 8 days.